Integrated redundancy and storage design optimization for reliable ASU based on Markov Chain - A Game Theoretic Solution

Yixin Ye,[†] Ignacio E. Grossmann,[*,†] Jose M. Pinto,[‡] and Sivaraman Ramaswamy[‡]

[†]*Department of Chemical Engineering, Carnegie Melon University, Pittsburgh, PA 15232*

[‡]*Business and Supply Chain Optimization, Linde.Digital, Linde plc, Tonawanda, NY 14150*

E-mail: grossmann@cmu.edu

Abstract

The profitability of a chemical plant is directly related to its reliability, which has always been a major concern in the chemical industry. In this paper, we address problem at the conceptual design phase of an air separation plant to minimize the negative income, which consists of the penalty incurred from pipeline supply interruption and the cost of increasing reliability, including having redundant units and storage tanks. An MILP model (denoted as RST) based on Markov Chain assumption is proposed, and applied to the motivating example of an air separation plant. Furthermore, in order to tackle larger superstructures, we propose a game theoretic algorithm that decomposes and restructures the problem as a team game of the individual processing stages and arrives at a Nash Equilibrium among them. It is also shown that a good initialization point close to the global optimum can be easily obtained, which guarantees the quality of the Nash Equilibrium solution. A number of examples are then shown to illustrate the proposed algorithm's ability to solve to the global optimality of

the original MILP model (RST) and to reach the solution in much shorter time than the original MILP model (RST).

Keywords: Reliability Design, Optimization, Markov Chain, MILP, Game Theory

1 Introduction

The reliability of a chemical plant is very important as it directly impacts customer service level and its economic performance. A plant with all the state-of-art technologies may not be able to generate the expected profits because of poor decision making regarding its reliability. In industrial practice, significant emphasis is placed on carrying out improved maintenance operations. There has also been academic research on quantifying and optimizing the maintenance efforts after the commissioning of a plant (e.g. see,[11],[9],[5],[3] and[1]).

However, prior to operations, the decisions regarding system reliability are equally worth of consideration in the conceptual design phase.[13,14] integrate flexibility and reliability in process design by deciding the reliability index of each piece of equipment.[6] incorporate several strategies in both design and operations toward more resilient chemical processes, including major failure proof strategy for process plants, which is to have redundancies for critical equipment. There is a clear trade-off when higher expected availability of the process requires greater capital investment.[7] provide a literature survey on optimal reliability design methods classified in terms of problem formulations and optimization techniques.[2] address reliability in utility plant design and operation by considering a few pre-specified alternatives for redundancy selection, and for which they formulate an MILP model considering certain failure scenarios.[16] propose a general mixed-integer programming framework for the optimal selection of redundant units.

Another widely used strategy to improve product availability is providing buffer storage for intermediate or final products, which again incurs costs of building the tanks and maintaining the stock that increases with the size of the storage tanks. In our earlier effort[17] to optimize redundancy selection together with maintenance policies, Markov Chain is used to

model the stochastic process of failures and repairs. This paper inherits the Markov Chain framework and takes a step back from unifying design and operations decisions to focus on expanding the scope of design decisions with the inclusion of storage tanks. For the ASU processes that motivated this work, it is especially important and common to have storage tanks of liquid products as the last line of defense because the penalty of interrupting pipeline supplies can be very large. In a most similar previous work,[12] optimize the reliable design of chemical sites networks with Markov Chain framework, and estimate the stochastic process of buffer storage consumption with the linear upper bound of its variance. As an improvement, this paper models the stochastic process exactly, which allows it to be associated with outage penalty and be reflected in the objective function.

The exact modeling of outage penalties provides a much closer representation of the trade-offs that decision makers face in reality, but it also results in nonlinear and non-convex constraints. Therefore, general decomposition methods like Lagrangean decomposition and Benders decomposition cannot be readily applied to the problem when we want to generalize the model and deal with larger superstructures. On the other hand, game theory provides an interesting view of decision making processes.[8] does an emergy analysis of industrial ecosystem that treats as players.[4] propose a consensual decision-making model based on game theory for LNG processes.[19] address both the cooperative and competitive properties of supply chain planning problems with a game theory approach. Inspired by these works, in this paper, we use the concept of team game to reach a local optimum from a good initialization point. It provides a novel perspective for the simultaneous optimal design of system redundancy and storage in respect to product availability, on top of the proposed general mixed integer formulation, where the stochastic process inferences of equipment failures and repairs are modeled in exact.

Section 2 introduces the motivating example of an ASU process and states the problem. In section 3, we develop the MILP model (RST) and reveal the fact that its computational complexity increases drastically with problem size. Section 4 presents the results of solving

the motivating example with (RST) as well as the computational difficulty of applying the model to a slightly enlarged example. In section 5, we introduce an iterative algorithm towards the team game Nash equilibrium, which is a necessary condition for the global optimum, and show that a good initial solution can be easily obtained for our problem, which guarantees the quality of the Nash equilibrium solution. Section 6 gives a step-by-step illustration of the algorithm by revisiting the enlarged problem first introduced in section 4. Section 7 show a series of examples for which all the global optima are obtained by the game theoretic approach in much shorter time than the original MILP model (RST).

2 Motivating example

Figure 1 shows a typical air separation facility that has two liquid product storage tanks for LO2 and LN2, respectively. When the ASU is down due to equipment failures, the liquid products can be vaporized to maintain pipeline supply. However, if the downtime is too long that the tank runs out before the ASU is back online, an interruption of pipeline supply is unavoidable. Typically, the gas supplier and the customers agree that interruption of pipeline supply leads to significant penalty on the supplier.

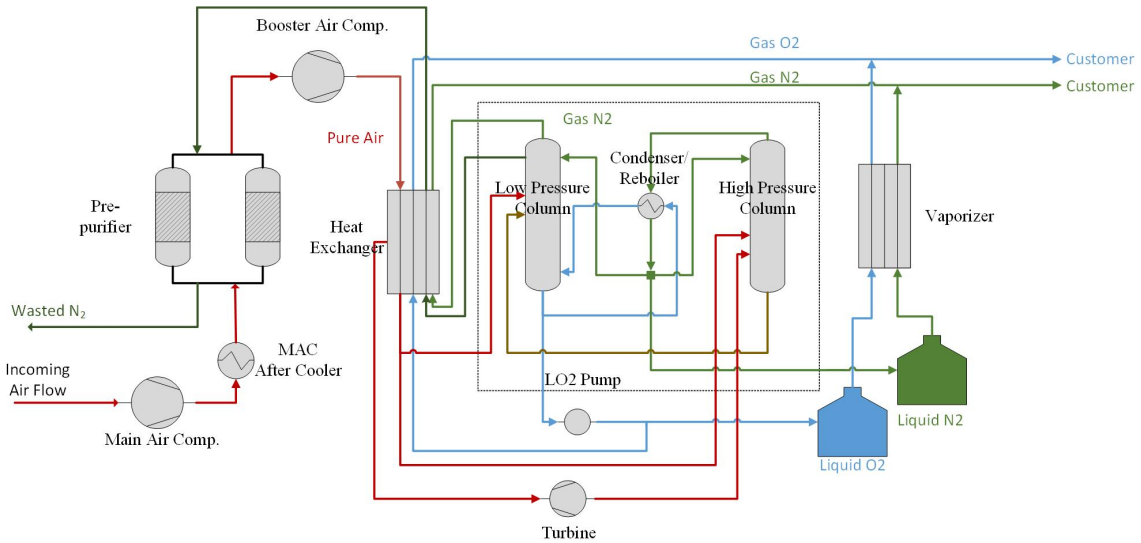

Figure 1: ASU with storage

Figure 2 shows the system superstructure. The purpose of the model is to determine the selection of parallel units among a finite number of possibly distinct candidates, and the sizes of the two liquid product storage tanks, in order to achieve the minimum cost balancing capital investment and the interruption penalty from the pipeline customers.

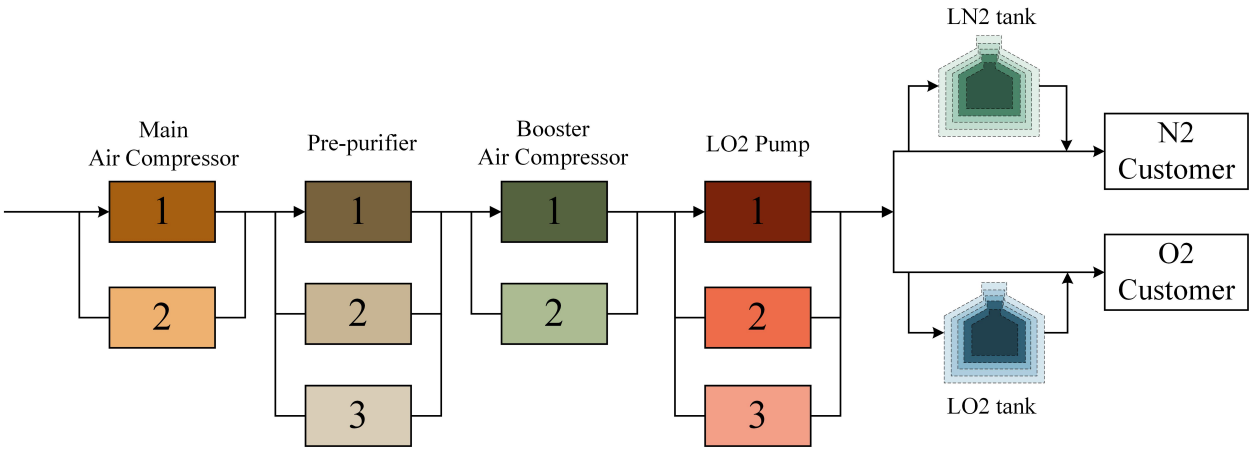

Figure 2: ASU with storage

3 Mathematical Model

The site is considered to have two parts, the air separation system with several stages in series, and the storage tanks. In section 3.1, the failure-repair process of the air separation system is modeled as a continuous-time Markov Chain depending on the system design, or redundancy selection. Next, in section 3.2, the impact of storage tank sizes on system availability is incorporated based on the relationships established in 3.1.

3.1 Modeling the processing system as a continuous-time Markov Chain

The processing stages, e.g. main air compressor, pre-purifier, are indexed with $k \in K$, whereas the individual potential redundancy designs in each stage are indexed with $h \in H_k$. Figure 3(a) shows a stage k with potentially 2 units to choose, while Figures 3(b), 3(c) and

3(d) show the three potential redundancy designs (selections) indexed by h, based on the superstructure.

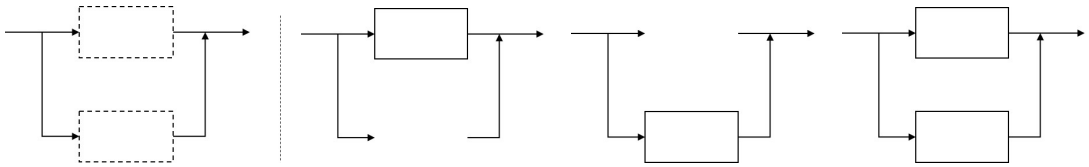

(a) Potential superstructure of the stage k (b) $h = 1$ (c) $h = 2$ (d) $h = 3$

Figure 3: The design options of individual stages

Binary variable $z_{k,h}$ indicates which design h is selected for stage k. Equation (1) requires that only one potential design is selected for each stage k. The investment cost of the design h in stage k is $\hat{C}^U_{k,h}$. Equation (2) calculates the investment cost of processing units depending on the design selection.

$$\sum_{h \in H_k} z_{k,h} = 1, \quad \forall k \in K \tag{1}$$

$$C^U = \sum_{k \in K} \sum_{h \in H_k} z_{k,h} \hat{C}^U_{k,h} \tag{2}$$

Based on the assumption that the time to failure and time to repair of single units follow exponential distributions, we model the failure-repair process of the processing stage k with design h as a continuous-time Markov Chain, and establish the corresponding transition matrix $\boldsymbol{W}_{k,h}$, from which two key quantities can be obtained: $\boldsymbol{\pi}_{k,h}$ is the probability distribution vector over the state space $S_{k,h}$ calculated from the corresponding transition matrix $\boldsymbol{W}_{k,h}$ with equation (3); $\boldsymbol{\sigma}_{k,h}$ is the diagonal of $\boldsymbol{W}_{k,h}$ as stated in equation (4). By the definition of continuous-time Markov Chain, the residence time of any state follows an exponential distribution. The physical meaning of $\sigma_{k,h}(s)$ is the rate parameter of that exponential distribution of state $s \in S_{k,h}$. For a thorough explanation of Markov Chain please refer to.[10] For the application of Markov Chain to redundancy systems please refer to our previous

paper.[17]

$$\boldsymbol{\pi}_{k,h}^{T} \cdot [\boldsymbol{W}_{k,h}, \mathbf{1}] = [\mathbf{0}^{T}, 1] \tag{3}$$

$$\boldsymbol{\sigma}_{k,h} = diag(\boldsymbol{W}_{k,h}) \tag{4}$$

With the stage level dynamics understood, we introduce the concept of system design, which is the combination of the individual stage designs. The set of all unique potential system designs is $\bar{H}$, and the elements are indexed by $\bar{h}$. Figure 4 shows the 9 possible system designs of a system with two stages just like the one stage shown in Figure 3(a).

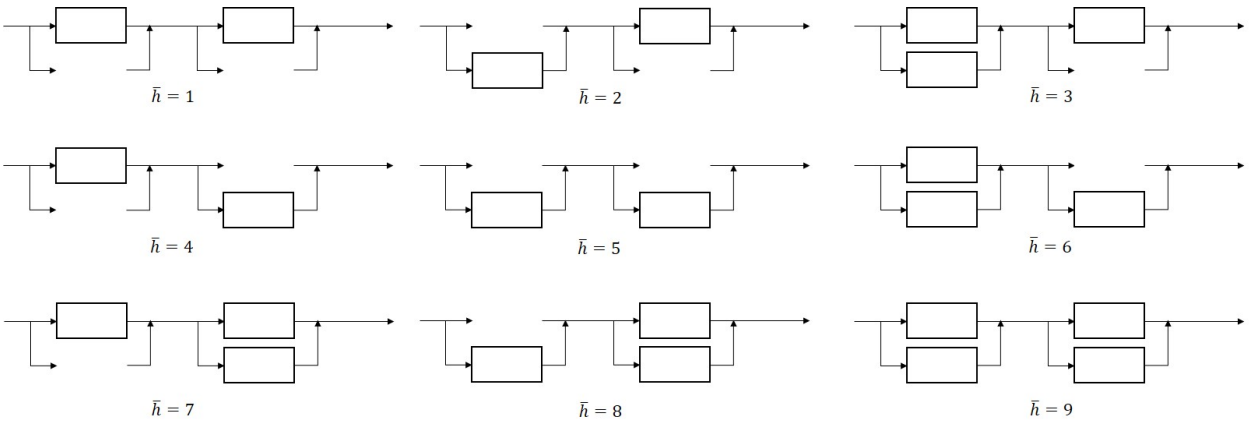

Figure 4: Potential system designs

Again, we model the failure-repair process of the system with design $\bar{h}$ as a continuous-time Markov Chain with transition matrix $\bar{\boldsymbol{W}}_{\bar{h}}$. $\boldsymbol{\pi}_{\bar{h}}$ is the probability distribution vector over the state space $\bar{S}_{\bar{h}}$ of the system design $\bar{h}$ calculated by equation (5). $\boldsymbol{\sigma}_{\bar{h}}$ is the diagonal of $\bar{\boldsymbol{W}}_{\bar{h}}$, and $\sigma_{\bar{h}}(\bar{s})$ is the rate parameter of the exponential distribution dictating the residence time of state $\bar{s} \in \bar{S}_{\bar{h}}$.

$$\bar{\boldsymbol{\pi}}_{\bar{h}}^{T} \cdot [\bar{\boldsymbol{W}}_{\bar{h}}, \mathbf{1}] = [\mathbf{0}^{T}, 1] \tag{5}$$

$$\bar{\boldsymbol{\sigma}}_{\bar{h}} = diag(\bar{\boldsymbol{W}}_{\bar{h}}) \tag{6}$$

In Appendix A we show that $\bar{\boldsymbol{\pi}}_{\bar{h}}$ and $\bar{\boldsymbol{\sigma}}_{\bar{h}}$ of system design $\bar{h}$ can be calculated based on $\boldsymbol{\pi}_{k,h}$ and $\boldsymbol{\sigma}_{k,h}$ as shown in (7) - (9), where design $h(k,\bar{h})$ in stage k is part of system design $\bar{h}$ (the $\prod\otimes$ represents Kronecker product. Please see Appendix A for illustration.).

$$\bar{\boldsymbol{\pi}}_{\bar{h}} = \boldsymbol{\pi}_{|K|,h(|K|,\bar{h})} \otimes ... \otimes \boldsymbol{\pi}_{2,h(2,\bar{h})} \otimes \boldsymbol{\pi}_{1,h(1,\bar{h})} \tag{7}$$

$$\bar{\boldsymbol{\sigma}}_{\bar{h}} = \sum_{k\in K} \mathbf{1}_{(g_k)} \otimes \boldsymbol{\sigma}_{k,h(k,\bar{h})} \otimes \mathbf{1}_{(l_k)} \tag{8}$$

g_k is the product of the state space dimensions of all the stages after stage k in the stage sequence, while l_k is the product of the state space dimensions of all the stages before k.

$$g_k = \prod_{(l,h):l>k,(l,h,\bar{h})\in HC} \|\boldsymbol{\pi}_{l,h}\|_0, \quad l_k = \prod_{(l,h):l<k,(l,h,\bar{h})\in HC} \|\boldsymbol{\pi}_{l,h}\|_0 \tag{9}$$

As mentioned above, $rt_{\bar{h}}(\bar{s})$, the residence time of state $\bar{s} \in \bar{S}_{\bar{h}}$, follows the exponential distribution with rate parameter $\bar{\sigma}_{\bar{h}}(\bar{s})$.

$$P(rt_{\bar{h}}(\bar{s}) = t) = \bar{\sigma}_{\bar{h}}(\bar{s})e^{-\bar{\sigma}_{\bar{h}}(\bar{s})t}, \quad \forall \bar{s} \in \bar{S}_{\bar{h}} \tag{10}$$

Finally we introduce $f_{\bar{h}}(\bar{s})$, the frequency of encountering each state $\bar{s}$. It is equal to the long term probability $\pi_{\bar{h}}(\bar{s})$ divided by the mean residence time $\overline{rt_{\bar{h}}}$, which is equal to the reciprocal of the rate parameter $\bar{\sigma}_{\bar{h}}(\bar{s})$.

$$f_{\bar{h}}(\bar{s}) = \frac{\pi_{\bar{h}}(\bar{s})}{\overline{rt_{\bar{h}}(\bar{s})}} = \pi_{\bar{h}}(\bar{s})\bar{\sigma}_{\bar{h}}(\bar{s}), \quad \forall \bar{s} \in \bar{S}_{\bar{h}} \tag{11}$$

3.2 System availability

In this section, we discuss how to incorporate the size of the storage tank for evaluating the network availability. The main idea is to calculate the frequency of the incidents where the plant is down due to unplanned equipment failure, and the downtime is so long that

the liquid storage runs out. Furthermore, we account for the proportional penalization in the objective function, because the actual penalty being paid to the customers is directly proportional to the frequency of supply interruption.

In section 3.1, it is established that the air separation system follows a continuous-time Markov Chain with transition matrix $\bar{\boldsymbol{W}}_{\bar{h}}$ for potential system design $\bar{h}$, which produces the stationary probability distribution $\bar{\pi}_{\bar{h}}(\bar{s})$ over the state space($\bar{S}_{\bar{h}}$), the residence time rate parameter $\bar{\sigma}_{\bar{h}}(\bar{s})$, and the frequency of encountering each state $f_{\bar{h}}(\bar{s})$.

We first focus on the random variable of the volume of liquid products decreasing during failure state $\bar{s} \in \bar{S}^f_{\bar{h}}$. It is proportional to the consumption rates δ^{LO2} or δ^{LN2}, and the random variable of the residence time $rt_{\bar{h}}(\bar{s})$. Based on the exponential distribution followed by $rt_{\bar{h}}(\bar{s})$ as shown in (10), they follow the exponential distribution with rate parameters $\frac{\bar{\sigma}_{\bar{h}}(\bar{s})}{\delta^{LO2}}$ or $\frac{\bar{\sigma}_{\bar{h}}(\bar{s})}{\delta^{LN2}}$.

$$P(V^{LO2dec}_{\bar{h}}(\bar{s}) = V) = \frac{\bar{\sigma}_{\bar{h}}(\bar{s})}{\delta^{LO2}} e^{-\frac{\bar{\sigma}_{\bar{h}}(\bar{s})}{\delta^{LO2}}V}, \quad \bar{s} \in \bar{S}^f_{\bar{h}} \tag{12}$$

$$P(V^{LN2dec}_{\bar{h}}(\bar{s}) = V) = \frac{\bar{\sigma}_{\bar{h}}(\bar{s})}{\delta^{LN2}} e^{-\frac{\bar{\sigma}_{\bar{h}}(\bar{s})}{\delta^{LN2}}V}, \quad \bar{s} \in \bar{S}^f_{\bar{h}} \tag{13}$$

We consider that there are a finite number of size options (k gallon) for both products, which we denote as V^{LO2}_n and V^{LN2}_n, with N^{LO2} and N^{LN2} as the index set of size options. x^{LO2}_n and x^{LN2}_n are binary variables that indicate the selection of tank sizes for LO2 (V^{LO2}_n) and LN2 (V^{LN2}_n), respectively. Equations (14) and (15) require that one and only one size is selected for each product.

$$\sum_{n \in N^{LO2}} x^{LO2}_n = 1 \tag{14}$$

$$\sum_{n \in N^{LN2}} x^{LN2}_n = 1 \tag{15}$$

C^T is the investment cost of storage tanks depending on their size selections.

$$C^T = \sum_{n \in N^{LO2}} x_n^{LO2} c_n^{LO2} + \sum_{n \in N^{LN2}} x_n^{LN2} c_n^{LN2} \tag{16}$$

Based on (11), (12) and (13). the outage frequencies of LO2 and LN2 for system design $\bar{h}$ and tank size n for the respective products, $\hat{fr}_{n,\bar{h}}^{LO2}$ and $\hat{fr}_{n,\bar{h}}^{LN2}$, can be calculated with (17) and (18).

$$\hat{fr}_{n,\bar{h}}^{LO2} = \sum_{\bar{s} \in \bar{S}_{\bar{h}}^f} f_{\bar{h}}(\bar{s}) \cdot P(V_{\bar{h}}^{LO2dec}(\bar{s}) \geq V_n^{LO2}) = \sum_{\bar{s} \in \bar{S}_{\bar{h}}^f} \bar{\pi}_{\bar{h}}(\bar{s}) \cdot \bar{\sigma}_{\bar{h}}(\bar{s}) \cdot e^{-\frac{V_n^{LO2}}{\delta^{LO2}} \bar{\sigma}_{\bar{h}}(\bar{s})} \tag{17}$$

$$\hat{fr}_{n,\bar{h}}^{LN2} = \sum_{\bar{s} \in \bar{S}_{\bar{h}}^f} f_{\bar{h}}(\bar{s}) \cdot P(V_{\bar{h}}^{LN2dec}(\bar{s}) \geq V_n^{LN2}) = \sum_{\bar{s} \in \bar{S}_{\bar{h}}^f} \bar{\pi}_{\bar{h}}(\bar{s}) \cdot \bar{\sigma}_{\bar{h}}(\bar{s}) \cdot e^{-\frac{V_n^{LN2}}{\delta^{LN2}} \bar{\sigma}_{\bar{h}}(\bar{s})} \tag{18}$$

The following constraints and disjuctions represent the relationship between the redundancy and storage selection and the expected outage penalties PN. In equation (19), T is the entire time horizon being considered. $penalty^{LO2}$ and $penalty^{LN2}$ are the amount of penalty per outage. Disjunctions (20)-(21) enforce that fr^{LO2} and fr^{LN2} are equal to the parameters $\hat{fr}_{n,\bar{h}}^{LO2}$ and $\hat{fr}_{n,\bar{h}}^{LN2}$ where the corresponding stage designs and storage tank sizes are selected.

$$PN = T(penalty^{LO2} \cdot fr^{LO2} + penalty^{LN2} \cdot fr^{LN2}) \tag{19}$$

$$\bigvee_{n \in N^{LO2}, \bar{h} \in \bar{H}} \begin{bmatrix} X_n^{LO2} \wedge (\bigwedge_{k \in K} Z_{k,h(k,\bar{h})}) \\ fr^{LO2} = \hat{fr}_{n,\bar{h}}^{LO2} \end{bmatrix} \tag{20}$$

$$\bigvee_{n \in N^{LN2}, \bar{h} \in \bar{H}} \begin{bmatrix} X_n^{LN2} \wedge (\bigwedge_{k \in K} Z_{k,h(k,\bar{h})}) \\ fr^{LN2} = \hat{fr}_{n,\bar{h}}^{LN2} \end{bmatrix} \tag{21}$$

We define the continuous variables $fr_{n,\bar{h}}^{LO2}$ and $fr_{n,\bar{h}}^{LN2}$ for the hull reformulation[15] into equa-

tions (22) - (28).

$$PN = T(penalty^{LO2} \cdot \sum_{n \in N^{LO2}} \sum_{\bar{h} \in \bar{H}} fr_{n,\bar{h}}^{LO2} + penalty^{LN2} \cdot \sum_{n \in N^{LN2}} \sum_{\bar{h} \in \bar{H}} fr_{n,\bar{h}}^{LN2}) \tag{22}$$

$$fr_{n,\bar{h}}^{LO2} \leq x_n^{LO2} \hat{fr}_{n,\bar{h}}^{LO2}, \quad \forall k \in K, n \in N^{LO2} \tag{23}$$

$$fr_{n,\bar{h}}^{LO2} \leq z_{k,h(k,\bar{h})} \hat{fr}_{n,\bar{h}}^{LO2}, \quad \forall n \in N^{LO2}, \bar{h} \in \bar{H} \tag{24}$$

$$fr_{n,\bar{h}}^{LO2} \geq (\sum_{k \in K} z_{k,h(k,\bar{h})} - |K| + x_n^{LO2}) \hat{fr}_{n,\bar{h}}^{LO2}, \quad \forall n \in N^{LO2}, \bar{h} \in \bar{H} \tag{25}$$

$$fr_{n,\bar{h}}^{LN2} \leq x_n^{LN2} \hat{fr}_{n,\bar{h}}^{LN2}, \quad \forall k \in K, n \in N^{LN2} \tag{26}$$

$$fr_{n,\bar{h}}^{LN2} \leq z_{k,h(k,\bar{h})} \hat{fr}_{n,\bar{h}}^{LN2}, \quad \forall n \in N^{LN2}, \bar{h} \in \bar{H} \tag{27}$$

$$fr_{n,\bar{h}}^{LN2} \geq (\sum_{k \in K} z_{k,h(k,\bar{h})} - |K| + x_n^{LN2}) \hat{fr}_{n,\bar{h}}^{LN2}, \quad \forall n \in N^{LN2}, \bar{h} \in \bar{H} \tag{28}$$

The objective function is (29).

$$\min_{z_{k,h}, x_n^{LO2}, x_n^{LN2}} \quad C^U + C^T + PN \tag{29}$$

To summarize, the model (ST) is an MILP minimizing the total cost (29) under the constraints (1), (2), (14)-(16), and (22)-(28). A hidden bottleneck of the model(ST) is the computation of the exponential number of parameters $\hat{fr}_{n,\bar{h}}^{LO2}$ and $\hat{fr}_{n,\bar{h}}^{LO2}$ (based on equations (3), (4), (7), (8), (17), and (18)) with respect to the size of the design superstructure. To illustrate, we consider a small example for the potential designs in Figure 4 with 3 possible sizes for LO2 and LN2 storage tanks. In order to determine the 18 parameters for each of the two groups $\hat{fr}_{n,\bar{h}}^{LO2}$ and $\hat{fr}_{n,\bar{h}}^{LO2}$, we have to solve for the probability vectors of 9 different state spaces of dimensions 4-25, before carrying out the calculation in (17) and (18) for the different tank sizes. Table 1 shows how the computation workload increases drastically as the superstructures grow in size. Specifically, to calculate a single parameter $\hat{fr}_{n,h}^{LO2}$, we need to find out the corresponding state space of potential design $\bar{h}$, and calculate $\bar{\boldsymbol{\pi}}_{\bar{h}}^T$ and $\bar{\boldsymbol{\sigma}}_{\bar{h}}^T$,

the complexity of which depends on the dimension of the state space. Therefore, not only the number of parameters increases with the size of the superstructure, but also the effort needed to determine each single parameter.

Table 1: Required computations for different superstructures

		SMALL	MEDIUM	LARGE
System statistics	Number of stages	2	3	4
	Number of potential units per stage	2	3	4
	Number of potential tank sizes	3	4	5
Computational tasks	Number of state space	9	343	50625
	Max dimension of state space	24	21870	141,087,744
	Number of parameters	36	2744	506250

4 Solution of the motivating problem and restrictions of the model (ST)

In this section, we present more details about the example shown in section 2, including the assigned parameters and corresponding solutions.

Table 2 shows the failure modes considered for each processing stage. The mean time between failures (MTBF) and the mean time to repair (MTTR) are known for each failure mode. The failure rates and repair rates can be obtained by taking their respective reciprocals. The transition matrices are obtained as discussed in our previous work[17]. The mean time between failures (MTBF) ranges from 5 to 25 years. Mean time to repair (MTTR) ranges from 8 to 1080 hours.

Table 2: Failure modes of each processing stage

Stage	Failure mode	Stage	Failure mode	Stage	Failure mode	Stage	Failure mode
Main air compressor	FMC1 FMC2 FMC3 FMC4 FMC5 FMC6	Pre-purifier	FMPF1	Booster air compressor	FMC1 FMC2 FMC3 FMC4 FMC5 FMC6	LO_2 Pump	FMP1

The capital cost of each unit ranges from \$140k to \$1250k. Table 3 shows the penalty rates and pipeline flow rates used in the model.

Table 3: Profitability parameters

$penalty^{LO2}$ (k\$ per outage)	$penalty^{LN2}$ (k\$ per outage)	δ^{LO2} (k gallon per day)	δ^{LN2} (k gallon per day)
2000	2000	48	60

Table 4 shows the tank size options and corresponding costs for LO2 and LN2 storage. LO2 tanks are generally more expensive.

Table 4: Tank size options and costs

Size options (k gallon)	100	400	700	1000	1500
Price for LO2 (k\$)	55	237	427	621	951
Price for LN2 (k\$)	50	215	388	565	864

The MILP model (ST) has 8828 equations and 2800 variables, with 269 of them being binary variables. The parameters are calculated in Python and the model is solved with CPLEX 12.8.0.0 in Pyomo. The total time to calculate the parameters and solving the model is 8.0s, where 5.3s is used for parameter calculation, and 2.7s for solving the MILP. The optimal design is shown in Figure 5. The expected frequency of LO2 outage is 0.005732

in the 10 year horizon, which incurs $11,464 penalty. The expected frequency of LN2 outage is 0.006 in the 10 year horizon, which incurs $12,291 penalty.

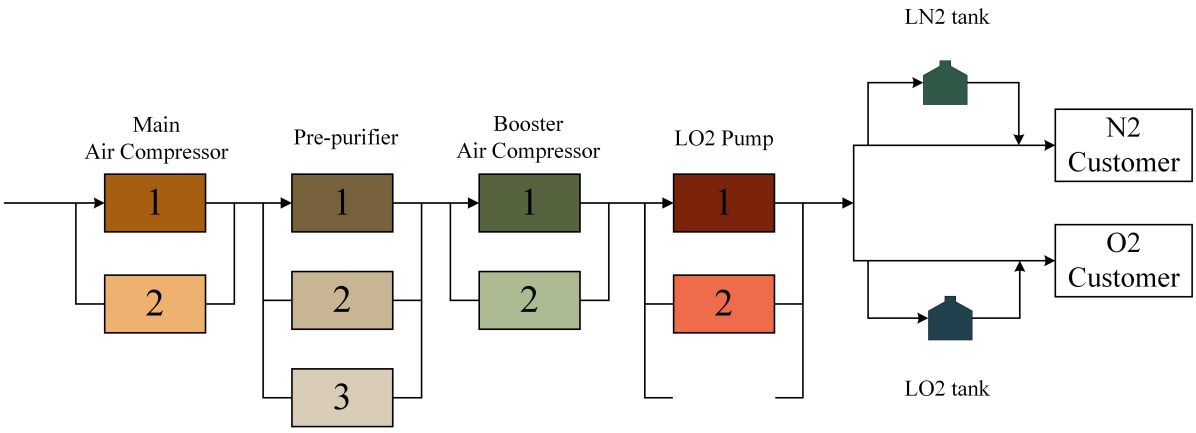

Figure 5: ASU with storage

As mentioned in section 3.2, it becomes more challenging to enumerate all possible combinations of $(n, \bar{h})$ and calculate $\hat{fr}^{LO2}_{n,\hat{h}}$ and $\hat{fr}^{LN2}_{n,\bar{h}}$ as the number of stages and potential units increase. In fact, for a larger problem where there are one more potential units for each of first three stages, the computational time of (ST) is 2053.5s, out of which 1697.2s are used for the parameter calculation. Moreover, for the example presented above, the total number of complicating parameters is 2520, and the maximum scenario number to consider for each parameter is 4536, while for the larger problem, those numbers become 37730 and 14,117,880, respectively.

5 Iterative game-theoretic algorithm

In order to overcome the bottleneck of the exponential parameter computational time, we propose an algorithm that starts with approximate and incomplete parameters, and iteratively adjusts the parameter pool as appropriate while the models are being solved, which allows us to achieve a Nash equilibrium, or a "person-by-person" optimum, among the stages.

The analogy of the problem being addressed to a team game is as follows. Each stage has its own contribution to the system costs by adding capital costs as well as the penalties from

unplanned downtimes. The condition of each stage (selection of parallel units) impacts its contribution to the penalties, just like each player is largely responsible for his/her contribution to the team performance. However, they play as a team in the sense that the individual contributions to the penalties (if a failure is due to a specific stage, the resulting downtime is considered its contribution) can be slightly affected by the conditions of the other stages. To be more specific, a failure of one stage means the failure of the entire system. Therefore, the extents of reliability and investment levels have to be balanced among the stages. For example, it might not be favorable to have one stage being much more reliable than the others, even if it is the best solution for itself standing alone. It is because the other stages are more likely to fail before it does and cover its failures, and therefore, the marginal decrease in its contribution to the system failure from increasing reliability investment is less than the case where this stage forms a one-stage-system.

The problem can be viewed as a team game[18] where the players are the $|K|$ stages. Inequality (30) shows the definition of Nash equilibrium in a team game: Given the strategy of all other players $\rho' \in \mathcal{P}$(the design selection of all other stages $l \in K, l \neq k$), there is no other strategy $\xi'_\rho \in \Xi_\rho$ (potential design h) for any single player $\rho \in \mathcal{P}$ (single stage k) that could give better utility C (lower objective function values):

$$C(\xi^*_1, ..., \xi^*_\rho, \xi^*_{|\mathcal{P}|}) \leq C(\xi^*_1, ..., \xi'_\rho, \xi^*_{|\mathcal{P}|}), \quad \forall \rho \in \mathcal{P}, \xi'_\rho \in \Xi_\rho \tag{30}$$

Before going into the details of the proposed algorithm, we will graphically illustrate its significance of reducing parameter calculation efforts by considering a small system as shown in Figure 6. The three rectangles grouping three dots of different sizes represent three stages each with three design options. The original formulation (RST) requires calculating the parameters for each valid combination (27 triangles that have one vertex in each rectangle).

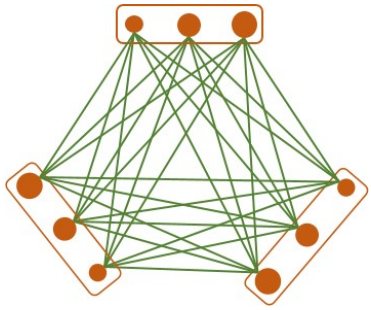

Figure 6: Original way has to calculate everything in advance

However, in Figures 7, 8, and 9, which represent the steps in the proposed algorithm, the connecting segments can be much sparser, since much fewer parameters need to be calculated following the proposed algorithm pursuing a Nash equilibrium.

First we optimize the stage-wise design selection with approximated impact from other stages. The approximation effort is presented in detail in section 5.1. The triangle in Figure 7 stands for the selected designs for individual stages.

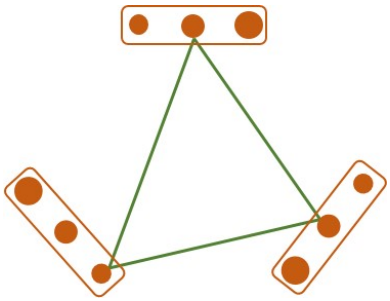

Figure 7: Initial approximated optimum

An equilibrium test is then performed to this group of design to determine whether any single stage has a superior deviation (deviation that generates lower total cost) given that the rest of the stages stick to the current plan. As shown in Figure 8, the solid triangle represents the group of design undergoing the equilibrium test following from Figure 7. In each rectangle group of dots, the 2 dots supporting dashed vertices represent the deviations being examined, which oppose the solid sides, as the deviations are taken with the rest of the stages unchanged and unaffected.

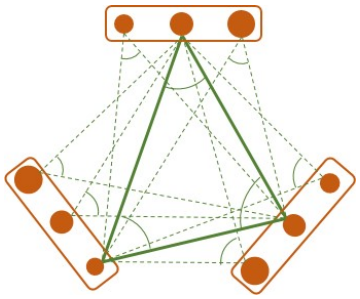

Figure 8: Equilibrium checking

If there is no superior deviation to the current plan, then the current design is a Nash equilibrium point. If otherwise, for example, in Figure 9(a), the dot supporting the vertex with thinner sides is a superior deviation for the stage it belongs to, we go to the next step shown in Figure 9(b). In this step, we add all the design selections (the 6 triangles with 2 thin dashed sides) that can be obtained by mutating the current selection, to the pool of potential system designs, while removing the current selection itself (the triangle with all thick dashed sides).

It is worth noting the difference between the 6 vertices supported by dashed sides in Figure 8 and the 6 dashed triangles in Figure 9(b): The dashed vertices are fictional deviations that affect the performance of the stage itself but not the outputs of the other stages(players), while a dashed triangle means that all the stages(players) take on a new set of designs(strategies) together, and the impacts on the outputs of each others are accounted for.

The optimal design in the current pool will again go back through the equilibrium check stage like in Figure 8, until a Nash equilibrium point is found.

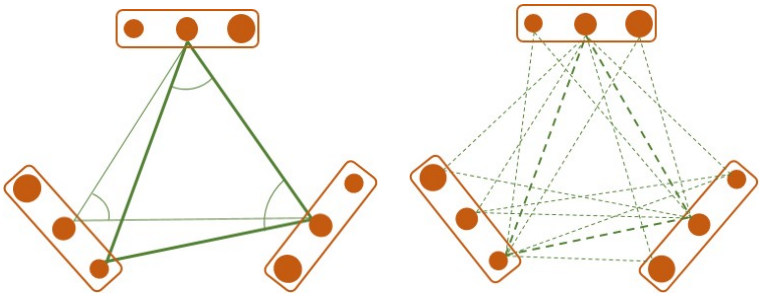

(a) Superior deviation found (b) Mutate and optimize

Figure 9

We can see that the new algorithm reduces a large part of the parameter calculations compared to the original model, especially when the number of stages and potential designs increases. It is worth mentioning that an overall optimum implies a Nash equilibrium, but the reverse is not true. Therefore, the Nash equilibrium that we pursue in this method can be considered a sub-optimal solution or a local optimum.

In section 5.1, we first show how the complicating parameters, $\hat{fr}_{n,\bar{h}}^{LO2}$ and $\hat{fr}_{n,\bar{h}}^{LN2}$ in (17) and (18), can be closely approximated with much simpler expressions. Next we present a terms rearrangement that breaks down the summations over system failure states according to the exact stage where the failure is happening, which reveals a linear impact of the other stages on the contribution to liquid-over-consumption of each individual stages. In section 5.2, we present a step-by-step description of the algorithm.

5.1 Approximation and rearrangement of key parameter expression

In this section, we propose an approximate expression and a rearranged expression of the key parameters, the outage frequencies of the liquid products (LO2 and LN2) output, $\hat{fr}_{n,\bar{h}}^{LO2}$ and $\hat{fr}_{n,\bar{h}}^{LN2}$, which is in preparation for the iterative solution scheme explained in the next section. In the following context, we only focus on LO2 and omit the similar term rearrangements and approximations that are also done for LN2 to avoid unnecessary repetition.

First, we rearrange the expression in (31) with the following notations:

For each stage k, we let $\tilde{h}$ index the potential designs of the complementary subsystem obtained by subtracting stage k from the entire system. For example, as shown in Figure 10, in the perspective of stage 1, the complementary subsystem refers to the system consists of stages 2 and 3. Similarly to $h(k, \bar{h})$, we define $\tilde{h}(k, \bar{h})$ as the index of the potential complementary design of stage k that is part of system design $\bar{h}$.

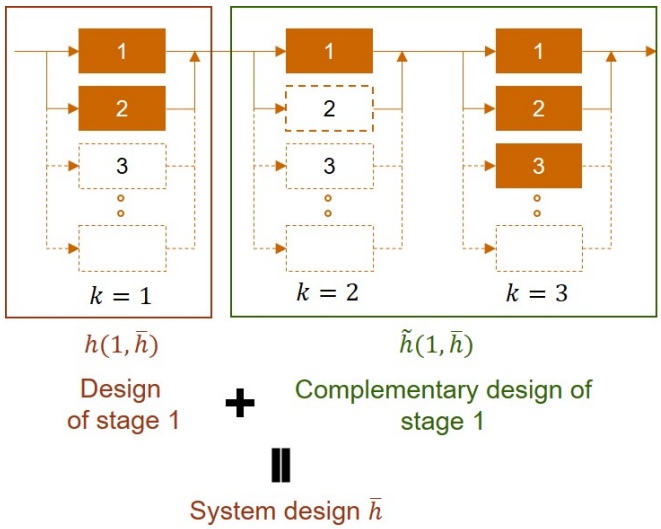

Figure 10: From the perspective of stage 1

In the original expression shown in (17), the system failure scenarios are directly enumerated, whereas in (31), the summation over the system failure scenarios breaks down by the stage k that causes the failure (see Appendix B for detailed derivation).

$$\hat{fr}_{n,\bar{h}}^{LO2} = \sum_{k \in K} \sum_{s \in S^f_{k,h(k,\bar{h})}} [\pi_{k,h(k,\bar{h})}(s) \cdot e^{-\frac{V_n^{LO2}}{\delta^{LO2}} \sigma_{k,h(k,\bar{h})}(s)} \cdot \sigma_{k,h(k,\bar{h})}(s) \cdot \sum_{\tilde{s} \in \tilde{S}_{k,\tilde{h}(k,\bar{h})}} \tilde{\pi}_{k,\tilde{h}(k,\bar{h})}(\tilde{s}) \cdot e^{-\frac{V_n^{LO2}}{\delta^{LO2}} \tilde{\sigma}_{k,\tilde{h}(k,\bar{h})}(\tilde{s})} \cdot (1 + \frac{\tilde{\sigma}_{k,\tilde{h}(k,\bar{h})}(\tilde{s})}{\sigma_{k,h(k,\bar{h})}(s)})] \tag{31}$$

We denote the stage-wise component of $\hat{fr}_{n,\bar{h}}^{LO2}$ as $\hat{FR}_{n,k,h(k,\bar{h})}^{LO2}$:

$$\hat{fr}_{n,\bar{h}}^{LO2} = \sum_{k \in K} \hat{FR}_{n,k,h(k,\bar{h})}^{LO2} \tag{32}$$

After rearrangement, $\hat{FR}_{n,\bar{h}}^{LO2}$ has the exact expression as shown in (33).

$$\hat{FR}_{n,k,h(k,\bar{h})}^{LO2} = \Theta_{n,k,h(k,\bar{h})}^{LO2} \cdot \Phi_{n,k,\tilde{h}(k,\bar{h})}^{LO2} + \Phi_{n,k,h(k,\bar{h})}^{LO2} \cdot \Theta_{n,k,\tilde{h}(k,\bar{h})}^{LO2}, \tag{33}$$

where

$$\Theta_{n,k,h}^{LO2} = \sum_{s \in S_{k,h}^{f}} \pi_{k,h}(s) \cdot e^{-\frac{V_n^{LO2}}{\delta^{LO2}} \sigma_{k,h}(s)} \cdot \sigma_{k,h}(s) \tag{34}$$

$$\Phi_{n,k,\tilde{h}}^{LO2} = \sum_{\tilde{s} \in \tilde{S}_{k,\tilde{h}}} \tilde{\pi}_{k,\tilde{h}}(\tilde{s}) \cdot e^{-\frac{V_n^{LO2}}{\delta^{LO2}} \tilde{\sigma}_{k,\tilde{h}}(\tilde{s})} \tag{35}$$

$$\Phi_{n,k,h}^{LO2} = \sum_{s \in S_{k,h}^{f}} \pi_{k,h}(s) \cdot e^{-\frac{V_n^{LO2}}{\delta^{LO2}} \sigma_{k,h}(s)} \tag{36}$$

$$\Theta_{n,k,\tilde{h}}^{LO2} = \sum_{\tilde{s} \in \tilde{S}_{k,\tilde{h}}} \tilde{\pi}_{k,\tilde{h}}(\tilde{s}) \cdot e^{-\frac{V_n^{LO2}}{\delta^{LO2}} \tilde{\sigma}_{k,\tilde{h}}(\tilde{s})} \cdot \tilde{\sigma}_{k,\tilde{h}}(\tilde{s}) \tag{37}$$

Therefore, instead of enumerating by system designs $\bar{h}$, we focus on one stage k at a time and enumerate by its potential designs $h \in H_k$ and the potential complementary designs $\tilde{h} \in \tilde{H}_k$, and define $\hat{FR}_{n,k,h,\tilde{h}}^{LO2}$:

$$\hat{FR}_{n,k,h,\tilde{h}}^{LO2} = (\Theta_{n,k,h}^{LO2} \cdot \Phi_{n,k,\tilde{h}}^{LO2} + \Phi_{n,k,h}^{LO2} \cdot \Theta_{n,k,\tilde{h}}^{LO2}) \tag{38}$$

It is also shown in Appendix B that following from (31), (39) and (40) are based on the assumption that the failure rates are of the order of magnitude 10^{-4}, and the repair rates

are of 10^{-2}.

$$\hat{fr}_{n,\bar{h}}^{LO2} = \sum_{k\in K} \sum_{s\in S^f_{k,h(k,\bar{h})}} \pi_{k,h(k,\bar{h})}(s) \cdot e^{-\frac{V_n^{LO2}}{\delta^{LO2}}\sigma_{k,h(k,\bar{h})}(s)} \cdot \sigma_{k,h(k,\bar{h})}(s) \cdot (1 \pm O(10^{-2})) \tag{39}$$

$$\hat{FR}_{n,k,h(k,\bar{h})}^{LO2} = \Theta_{n,k,h(k,\bar{h})}^{LO2} \cdot (1 \pm O(10^{-2})) \tag{40}$$

Therefore, as shown in (40), we can use the sum of the outage frequencies of each stage alone $\sum_{k\in K} \Theta_{n,k,h(k,\bar{h})}^{LO2}$ to approximate the system outage frequency $\hat{fr}_{n,\bar{h}}^{LO2}$.

As mentioned at the beginning of this section, similar term rearrangements and approximations are done for LN2, which are omitted to avoid unnecessary repetition. To summarize, it is proposed to rewrite the original expression shown in (17) as (41) and approximate $\hat{fr}_{n,\bar{h}}^{LO2}$ with (42)..

$$\hat{fr}_{n,\bar{h}}^{LO2} = \sum_{k\in K} \hat{FR}_{n,k,h(k,\bar{h}),\tilde{h}(k,\bar{h})}^{LO2} \tag{41}$$

$$\hat{fr}_{n,\bar{h}}^{LO2} \approx \sum_{k\in K} \Theta_{n,k,h(k,\bar{h})}^{LO2} \tag{42}$$

5.2 Algorithm description

In this section, we provide a step-by-step description of the algorithm with reference to the above mathematical details and qualitative explanations. Briefly speaking, the algorithm takes advantage of the fact that the individual contribution from each stage is under limited impact of the other stages, and obtains a good initial solution ignoring these interrelations. It then iterates between two tasks, checking the equilibrium condition of a current design, and until confirming an equilibrium point, expanding the solution pool with all the mutations of unsuccessful previous designs to find a better design.

Step 1. Calculate $\Theta_{n,k,h}^{LO2}$ and $\Phi_{n,k,h}^{LO2}$ (first defined in (34) and (36)). Solve the MILP independent design selection problem (IDS) defined below, featuring the approximated pa-

rameters $\Theta^{LO2}_{n,k,h}$ and $\Theta^{LN2}_{n,k,h}$. Based on the relationship shown in (42), the MILP (IDS) is an approximation of (RST).

$$
\begin{aligned}
(IDS): \quad \min_{z_{k,h}, x_n^{LO2}, x_n^{LN2}} \quad & C^U + C^T + PN && (43)\\
\text{s.t.} \quad & \sum_{h \in H_k} z_{k,h} \geq 1, \quad \forall k \in K \\
& C^U = \sum_{k \in K} \sum_{h \in H_k} z_{k,h} \hat{C}^U_{k,h} \\
& \sum_{n \in N^{LO2}} x_n^{LO2} \geq 1 \\
& \sum_{n \in N^{LN2}} x_n^{LN2} \geq 1 \\
& C^T = \sum_{n \in N^{LO2}} x_n^{LO2} c_n^{LO2} + \sum_{n \in N^{LN2}} x_n^{LN2} c_n^{LN2} \\
& fr^{LO2}_{n,k,h} \leq z_{k,h} \Theta^{LO2}_{n,k,h}, \quad \forall n \in N^{LO2}, k \in K, h \in H_k \\
& fr^{LO2}_{n,k,h} \leq x_n^{LO2} \Theta^{LO2}_{n,k,h}, \quad \forall n \in N^{LO2}, k \in K, h \in H_k \\
& fr^{LO2}_{n,k,h} \geq (z_{k,h} + x_n^{LO2} - 1) \Theta^{LO2}_{n,k,h}, \quad \forall n \in N^{LO2}, k \in K, h \in H_k \\
& fr^{LN2}_{n,k,h} \leq z_{k,h} \Theta^{LN2}_{n,k,h}, \quad \forall n \in N^{LN2}, k \in K, h \in H_k \\
& fr^{LN2}_{n,k,h} \leq x_n^{LN2} \Theta^{LN2}_{n,k,h}, \quad \forall n \in N^{LN2}, k \in K, h \in H_k \\
& fr^{LN2}_{n,k,h} \geq (z_{k,h} + x_n^{LN2} - 1) \Theta^{LN2}_{n,k,h}, \quad \forall n \in N^{LN2}, k \in K, h \in H_k \\
& PN = T(penalty^{LO2} \cdot \sum_{n \in N^{LO2}} \sum_{k \in K} \sum_{h \in K_h} fr^{LO2}_{n,k,h} \\
& + penalty^{LN2} \cdot \sum_{n \in N^{LN2}} \sum_{k \in K} \sum_{h \in K_h} fr^{LN2}_{n,k,h}) \\
& c^U, c^T, PN \geq 0 \\
& z_{k,h} \in \{0,1\}, \forall k \in K, h \in H_k \\
& x_n^{LO2} \in \{0,1\}, \forall n \in N^{LO2} \\
& x_n^{LN2} \in \{0,1\}, \forall n \in N^{LN2}
\end{aligned}
$$

The optimal solution of (IDS) indicates the potential design to select for each stage k: $\{h^*_{(0)}(k), k \in K\}$ (refer to the dots supporting the triangle in Figure 7). Appendix C shows an estimated bound of the gap between the global optimum and the objective function resulting from k: $\{h^*_{(0)}(k), k \in K\}$ and the best storage selections that go with it.

Step 2. For each stage $k \in K$, solve the MILP equilibrium checking problems $(\text{ECP})_{(m,k)}$. m starts counting at $m = 1$. The model formulation is shown in (45). In order to do that ,we have to first calculate the parameters $\hat{FR}^{LO2}_{n,k,h,m}$ based on $\{h^*_{(m-1)}(k), k \in K\}$ as shown in (44) (refer to the dashed vertices in Figure 8).

$$\hat{FR}^{LO2}_{n,k,h,m} = \Theta^{LO2}_{n,k,h} \cdot \Phi^{LO2}_{n,k,\tilde{h}^*_{(m-1)}(k)} + \Phi^{LO2}_{n,k,h} \cdot \Theta^{LO2}_{n,k,\tilde{h}^*_{(m-1)}(k)} \tag{44}$$

$$(ECP)_{(m,k)}: \quad \min_{z_{k,h},x_n^{LO2},x_n^{LN2}} \quad C^U + C^T + PN \tag{45}$$

$$\text{s.t.} \sum_{h\in H_k} z_{k,h} \geq 1, \quad \forall k \in K$$

$$C^U = \sum_{h\in H_k} z_{k,h}\hat{C}^U_{k,h} + \sum_{l\in K\setminus\{k\}} \sum_{h\in H_l} \hat{C}^U_{l,h^*_{(m-1)}(l)}$$

$$\sum_{n\in N^{LO2}} x_n^{LO2} \geq 1$$

$$\sum_{n\in N^{LN2}} x_n^{LN2} \geq 1$$

$$C^T = \sum_{n\in N^{LO2}} x_n^{LO2} c_n^{LO2} + \sum_{n\in N^{LN2}} x_n^{LN2} c_n^{LN2}$$

$$fr^{LO2}_{n,k,h,m} \leq z_{k,h}\hat{FR}^{LO2}_{n,k,h,m}, \quad \forall n \in N^{LO2}, h \in H_k$$

$$fr^{LO2}_{n,k,h,m} \leq x_n^{LO2}\hat{FR}^{LO2}_{n,k,h,m}, \quad \forall n \in N^{LO2}, h \in H_k$$

$$fr^{LO2}_{n,k,h,m} \geq (z_{k,h} + x_n^{LO2} - 1)\hat{FR}^{LO2}_{n,k,h,m}, \quad \forall n \in N^{LO2}, h \in H_k$$

$$fr^{LO2}_{n,l,h,m} = 0, \quad \forall n \in N^{LO2}, l \in K \setminus \{k\}, h \in H_l \setminus \{h^*_{(m-1)}(k)\}$$

$$fr^{LO2}_{n,l,h,m} = x_n^{LO2}\hat{FR}^{LO2}_{n,l,h,m},$$

$$\forall n \in N^{LO2}, l \in K \setminus \{k\}, h \in H_l \setminus \{h^*_{(m-1)}(k)\}$$

$$fr^{LN2}_{n,k,h,m} \leq z_{k,h}\hat{FR}^{LN2}_{n,k,h,m}, \quad \forall n \in N^{LN2}, h \in H_k$$

$$fr^{LN2}_{n,k,h,m} \leq x_n^{LN2}\hat{FR}^{LN2}_{n,k,h,m}, \quad \forall n \in N^{LN2}, h \in H_k$$

$$fr^{LN2}_{n,k,h,m} \geq (z_{k,h} + x_n^{LN2} - 1)\hat{FR}^{LN2}_{n,k,h,m}, \quad \forall n \in N^{LN2}, h \in H_k$$

$$fr^{LN2}_{n,l,h,m} = 0, \quad \forall n \in N^{LN2}, l \in K \setminus \{k\}, h \in H_l \setminus \{h^*_{(m-1)}(k)\}$$

$$fr^{LN2}_{n,l,h,m} = x_n^{LNs2}\hat{FR}^{LN2}_{n,l,h,m},$$

$$\forall n \in N^{LN2}, l \in K \setminus \{k\}, h \in H_l \setminus \{h^*_{(m-1)}(k)\}$$

$$PN = T(penalty^{LO2} \cdot \sum_{n\in N^{LO2}} \sum_{k\in K} \sum_{h\in K_h} fr^{LO2}_{n,k,h,m}$$

$$+ penalty^{LN2} \cdot \sum_{n\in N^{LN2}} \sum_{k\in K} \sum_{h\in K_h} fr^{LN2}_{n,k,h,m})$$

$$c^U, c^T, PN \geq 0$$

$$z_{k,h} \in \{0,1\}, \forall k \in K, h \in H_k$$

$$x_n^{LO2} \in \{0,1\}, \forall n \in N^{LO2}$$

$$x_n^{LN2} \in \{0,1\}, \forall n \in N^{LN2}$$

The optimal solutions of the models $(\text{ECP})_{(m,k)}, k \in K$ indicate a group of design selection for each stage $\{h^{o}_{(m)}(k), k \in K\}$. If for every stage k, the complementary design indexed by (k, m) that was brought into $(\text{ECP})_{(m)}$ consists of the selected designs of the other stages, we say that a Nash equilibrium is found among the stages, and the iteration stops. Otherwise, go to step 3. The latter case is illustrated by Figure 9(a).

Step 3. Solve the MILP partial design selection model $(\text{PDS})_{(m)}$ shown in (49), which corresponds to the mutate and optimize step shown in Figure 9(b). The model is called partial because only an incomplete pool of possible designs are being evaluated. The associated parameters $\hat{C}^{U}_{\bar{h}}$, $\hat{fr}^{LO2}_{n,\bar{h}}$ and $\hat{fr}^{LN2}_{n,\bar{h}}$ are calculated in equations (46), (47) and (48). The index set $\bar{H}_{(m)}$ include the indices representing those system designs that for at least one stage, the complementary design is part of $\{h^{*}_{(m-1)}(k), k \in K\}$. In other words, the system designs to be included in the partial design selection model $(\text{PDS})_{(m)}$ are obtained by mutating the designs that are combinations of the stage designs in $\{h^{*}_{(m-1)}(k), k \in K\}$, which are represented by the dashed triangles in Figure 9(b). Some parameters from the last step can be reused here.

$$\hat{C}^{U}_{\bar{h}} = \sum_{k \in K} \hat{C}^{U}_{k,h(k,\bar{h})}, \quad \forall \bar{h} \in \bar{H}_{(m)} \tag{46}$$

$$\begin{aligned} \hat{fr}^{LO2}_{n,\bar{h}} &= \sum_{k \in K} \hat{FR}^{LO2}_{n,k,h(k,\bar{h}),\tilde{h}(k,\bar{h})} \\ &= \sum_{k \in K} (\Theta^{LO2}_{n,k,h(k,\bar{h})} \cdot \Phi^{LO2}_{n,k,\tilde{h}(k,\bar{h})} + \Phi^{LO2}_{n,k,h(k,\bar{h})} \cdot \Theta^{LO2}_{n,k,\tilde{h}(k,\bar{h})}), \quad n \in N^{LO2}, \bar{h} \in \bar{H} \end{aligned} \tag{47}$$

$$\hat{fr}_{n,\bar{h}}^{LN2} = \sum_{k\in K} \hat{FR}_{n,k,h(k,\bar{h}),\tilde{h}(k,\bar{h})}^{LN2}$$
$$= \sum_{k\in K} (\Theta_{n,k,h(k,\bar{h})}^{LN2} \cdot \Phi_{n,k,\tilde{h}(k,\bar{h})}^{LN2} + \Phi_{n,k,h(k,\bar{h})}^{LN2} \cdot \Theta_{n,k,\tilde{h}(k,\bar{h})}^{LN2}), \quad n \in N^{LN2}, \bar{h} \in \bar{H} \tag{48}$$

$$(PDS)_{(m)}: \quad \min_{z_{\bar{h}}, x_n^{LO2}, x_n^{LN2}} \quad C^U + C^T + PN \tag{49}$$
$$\text{s.t.} \sum_{\bar{h}\in\bar{H}_{(m)}} z_{\bar{h}} \geq 1, \quad \forall k \in K$$
$$C^U = \sum_{\bar{h}\in\bar{H}_{(m)}} z_{\bar{h}} \hat{C}_{\bar{h}}^U$$
$$\sum_{n\in N^{LO2}} x_n^{LO2} \geq 1$$
$$\sum_{n\in N^{LN2}} x_n^{LN2} \geq 1$$
$$C^T = \sum_{n\in N^{LO2}} x_n^{LO2} c_n^{LO2} + \sum_{n\in N^{LN2}} x_n^{LN2} c_n^{LN2}$$
$$fr_{n,\bar{h}}^{LO2} \leq z_{\bar{h}} \hat{fr}_{n,\bar{h}}^{LO2}, \quad \forall n \in N^{LO2}, \bar{h} \in \bigcup_{m'\leq m} \bar{H}_{(m')} \backslash \{\bar{h}_{(m')}^*, m' \leq m-1\}$$
$$fr_{n,\bar{h}}^{LN2} \leq z_{\bar{h}} \hat{fr}_{n,\bar{h}}^{LN2}, \quad \forall n \in N^{LN2}, \bar{h} \in \bigcup_{m'\leq m} \bar{H}_{(m')} \backslash \{\bar{h}_{(m')}^*, m' \leq m-1\}$$
$$PN = T(penalty^{LO2} \cdot \sum_{n\in N^{LO2}} \sum_{\bar{h}\in\bar{H}_{(m)}} fr_{n,\bar{h}}^{LO2}$$
$$+ penalty^{LN2} \cdot \sum_{n\in N^{LN2}} \sum_{\bar{h}\in\bar{H}_{(m)}} fr_{n,\bar{h}}^{LN2})$$
$$c^U, c^T, PN \geq 0$$
$$z_{\bar{h}} \in \{0,1\}, \forall \bar{h} \in \bar{H}_k$$
$$x_n^{LO2} \in \{0,1\}, \forall n \in N^{LO2}$$
$$x_n^{LN2} \in \{0,1\}, \forall n \in N^{LN2}$$

The optimal solution of $(\text{PDS})_{(m)}$ indicates the potential design to select for each stage k:

$\{h^*_{(m)}(k), k \in K\}$. After solving the model, let $m = m + 1$ and go back to step 2.

To reiterate, as shown in Figure 11, the algorithm iterates between two tasks, checking the equilibrium condition of $\{h^*_{(m)}(k), k \in K\}$, and finding a new design based on the unsuccessful previous solution and its superior deviation.

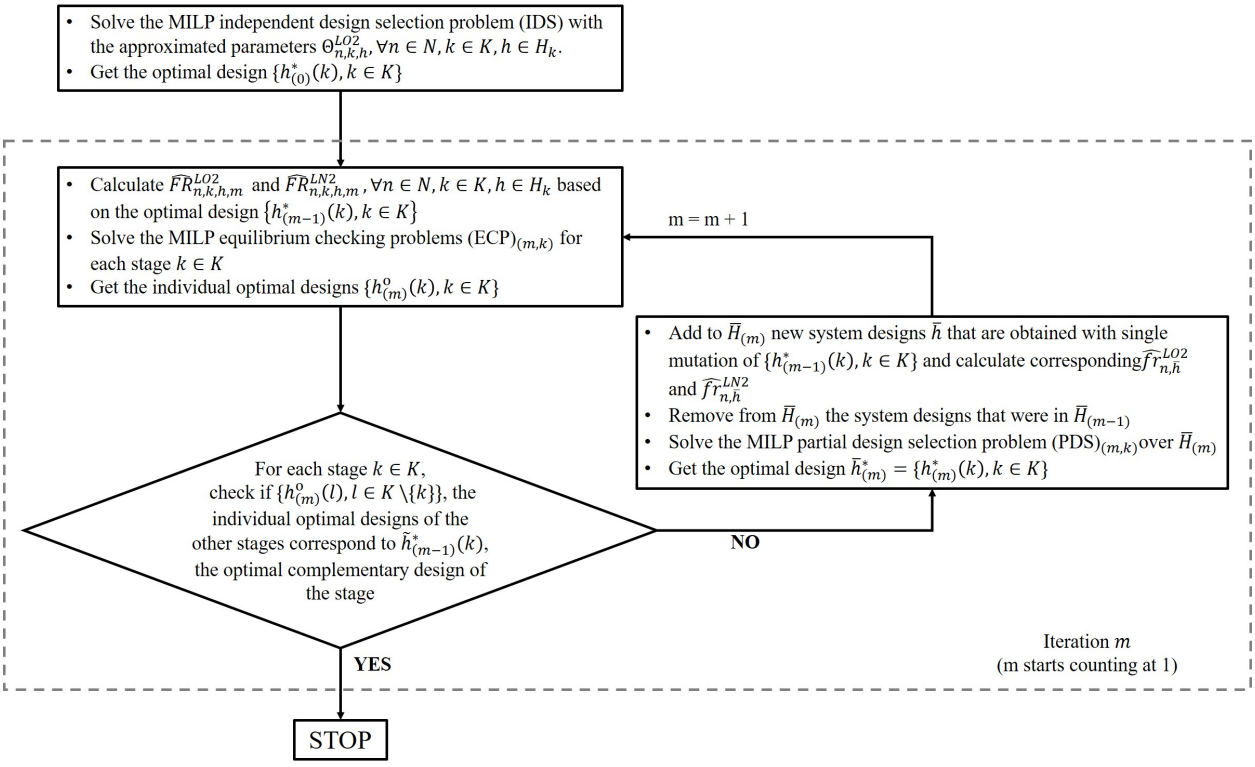

Figure 11: The flowchart of the iterative problem solving scheme

6 Illustration of the Algorithm

In order to better illustrate the algorithm, we solve again the enlarged problem discussed in section 2 and present the step-wise information. As shown in Figure 12, there is one more redundant unit to be chosen from for each of the first three stages. Reliability and cost data of each unit remain in the same range. The algorithm is able to find the optimum in 3 iterations.

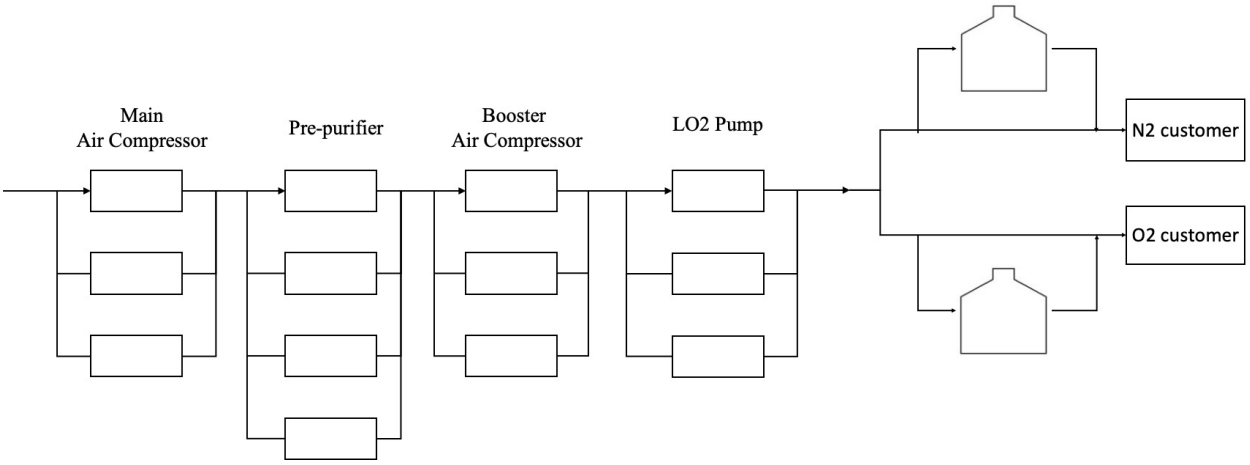

Figure 12: The enlarged superstructure

The initial design solution obtained from solving the MILP (IDS) (which has 363 variables with 32 binary variables, and 967 constraints) in step 1 is as shown in Figure 13, which is proven not to be a Nash equilibrium point among the stages in Step 2 by solving $(\text{ECP})_{(1)}$ (which has 363 variables with 32 binary variables, and 967 constraints). The estimate for LO2 penalty is \$10,327.9, and for LN2 penalty it is \$11,063.0, with the approximated parameters.

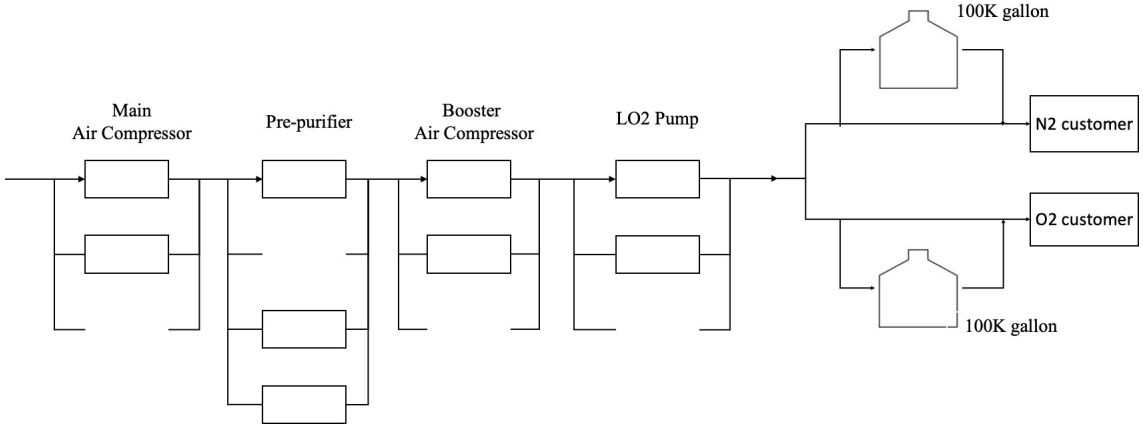

Figure 13: Initial design solution

Because a Nash equilibrium point is not found, we follow Step 3 to expand the solution pool by taking into consideration all possible redundancy selections that only differ from the initial design in one stage, at the same time, the initial design is permanently excluded. By solving The MILP model $(\text{PDS})_{(1)}$ (which has 330 variables with 29 binary variables, and

902 constraints), the best solution is as shown in Figure 14. The algorithm returns to Step 2 in iteration 2, and solves $(\text{ECP})_{(2)}$ (which has 363 variables with 32 binary variables, and 967 constraints) to find out that this is still not a Nash equilibrium point. The expected penalty from LO2 is \$11,477.2, while the expected penalty from LN2 is \$12,299.8.

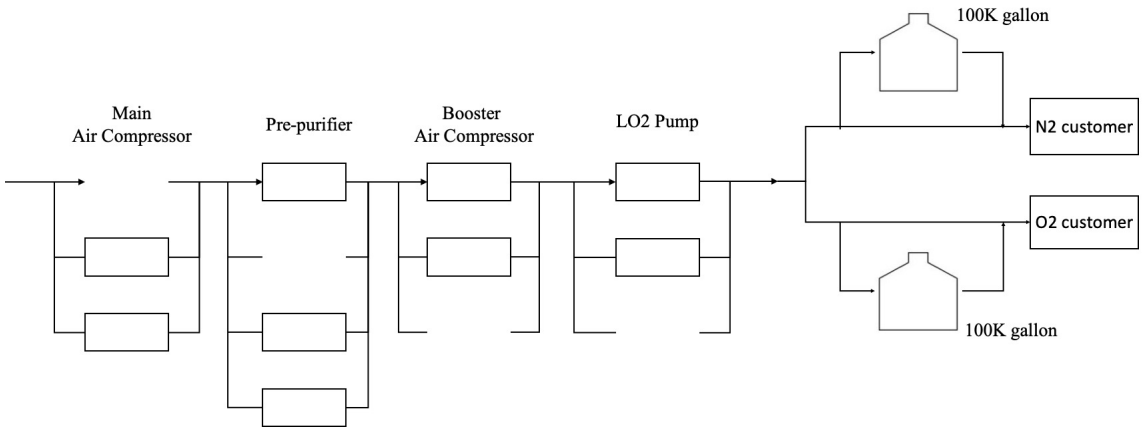

Figure 14: Best design after the first solution pool expansion

Therefore, we proceed to Step 3 in iteration 2 and expand the solution pool again by mutating only one stage at a time, and exclude the solution shown in Figure 14. The best solution solved by MILP model $(\text{PDS})_{(2)}$ (which has 561 variables with 50 binary variables, and 1553 constraints) is shown in Figure 15, which is checked out to be a Nash Equilibrium point. The expected penalty from LO2 is lowered by a small margin to \$11,468.5, similarly for LN2, the number becomes \$12,290.6. The original MILP formulation (RST) has 41546 variables, of which 3805 are binary, and 132063 constraints. It obtains the same result.

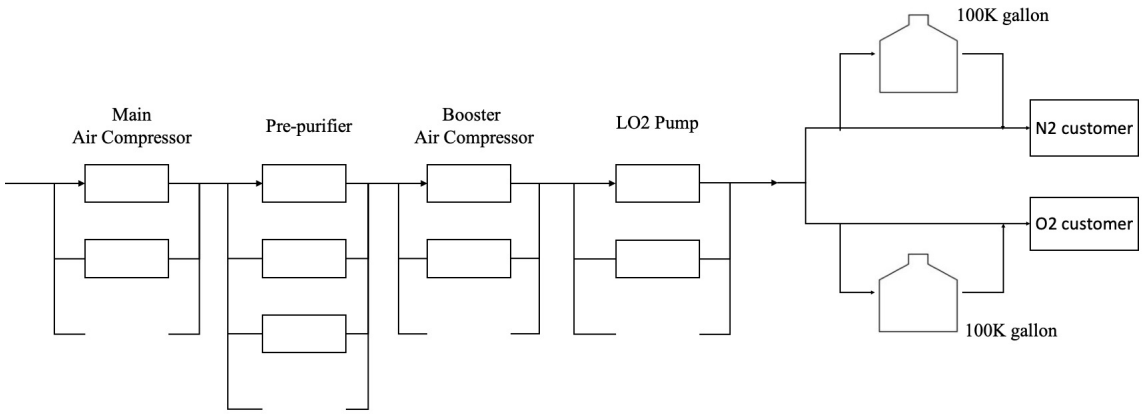

Figure 15: Best design after the second solution pool expansion

The total computational time is 7.9s, as opposed to 2053.5s if solved with the original formulation (RST) (that requires 1697.2 s for parameter calculation and 356.3 s for solution of the MILP).

7 More Examples

As was discussed in section 5.2, the globally optimal solution of the original formulation (RST) is a Nash-equilibrium solution but the reverse is not always true. However, we show in appendix C that, given that the failure rates and repair rates of the units are of certain orders of magnitudes, the gap between an easily obtained initial design and the global optimum is small and can be estimated, which makes it highly likely for the algorithm to arrive at the global optimum. In this section, we consider a example with the superstructure as shown in 16. It shares Table 2, Table 3 and Table 4 with the first example shown in section 4. Mean time between failure, Mean time to repair and capital costs are given in Table 5, which are not real world values and are only meant for illustrative purposes. A series of reliability parameters sensitivity tests are performed, for which the game-theoretic approach gives the global optima according to the solution of the original MILP (RST) (model stats), but in much shorter time.

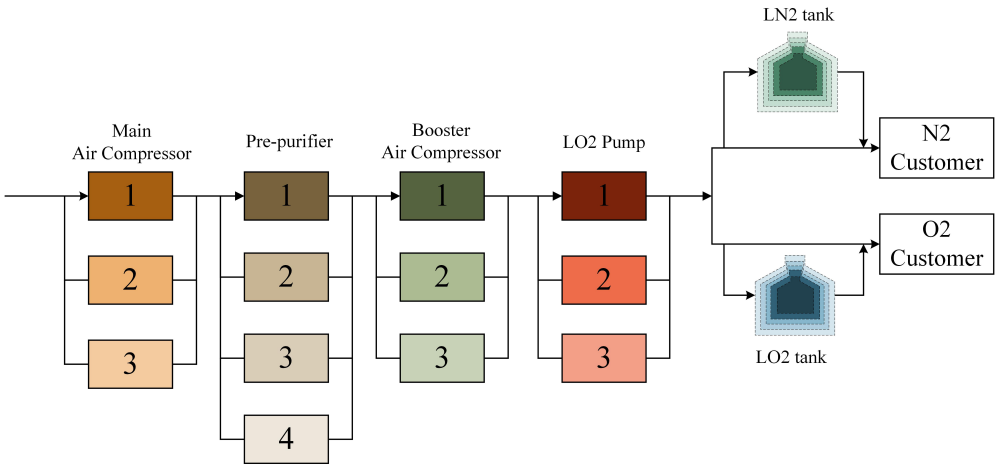

Figure 16: Design superstructure

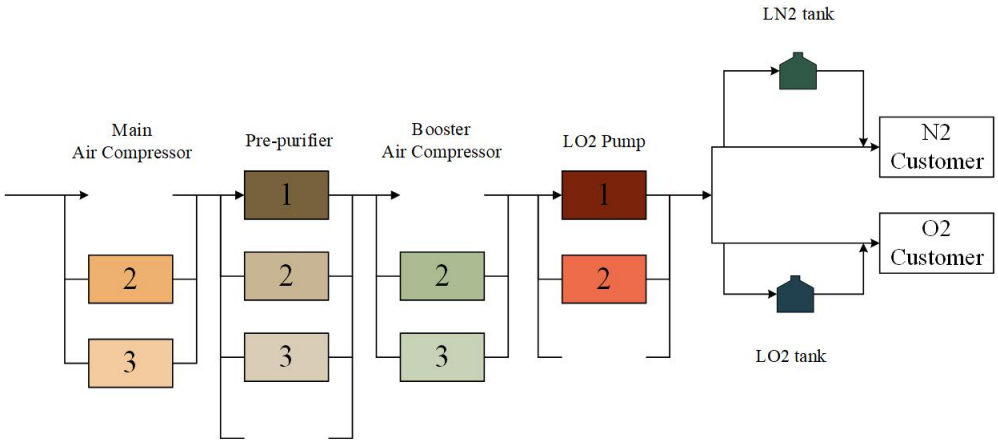

Figure 17: Optimal design for the parameters shown in the table

Figure 17 shows the optimal design. For both the main air compressor and the booster air compressor, units 2 and 3 are selected. The pre-purifier and the LO2 pump exclude the last potential units. The tanks for both LN2 and LO2 are of size 100k gallon. The capital cost on the processing equipment is \$6225k, while the capital cost on the storage tanks is \$105k. The expected frequency of LO2 outage is 0.0105 in the 10 year horizon, which incurs \$21,089 penalty. The expected frequency of LN2 outage is 0.0121 in the 10 year horizon, which incurs \$24,194 penalty.

Table 5: Reliability and installation cost parameters

Stage	Unit	Failure mode	$MTBF$ (day)	$MTTR$ (day)	Capital cost(k$)
Main air compressor	1	FMC1	5000	10	1250
		FMC2	3650	5	
		FMC3	7000	7	
		FMC4	1500	0.3	
		FMC5	5000	2	
		FMC6	7000	50	
	2	FMC1	5000	10	1240
		FMC2	3650	5	
		FMC3	5000	7	
		FMC4	1500	0.3	
		FMC5	6000	2	
		FMC6	6000	50	
	3	FMC1	4000	10	1200
		FMC2	4000	5	
		FMC3	4000	7	
		FMC4	1500	0.3	
		FMC5	5000	2	
		FMC6	6000	50	
Pre-purifier	1	FMPF1	3650	4	520
	2		3650	4	520
	3		3650	4	520
	4		3650	4	520
Booster air compressor	1	FMC1	5000	10	1000
		FMC2	3650	5	
		FMC3	7000	7	
		FMC4	1500	0.3	
		FMC5	5000	2	
		FMC6	7000	50	
	2	FMC1	5000	10	980
		FMC2	3650	5	
		FMC3	5000	7	
		FMC4	1500	0.3	
		FMC5	6000	2	
		FMC6	6000	50	
	3	FMC1	4000	10	950
		FMC2	4000	5	
		FMC3	4000	7	
		FMC4	1500	0.3	
		FMC5	5000	2	
		FMC6	6000	50	
LO_2 Pump	1	FMP1	3650	4	150
	2		3650	4	150
	3		3650	4	150

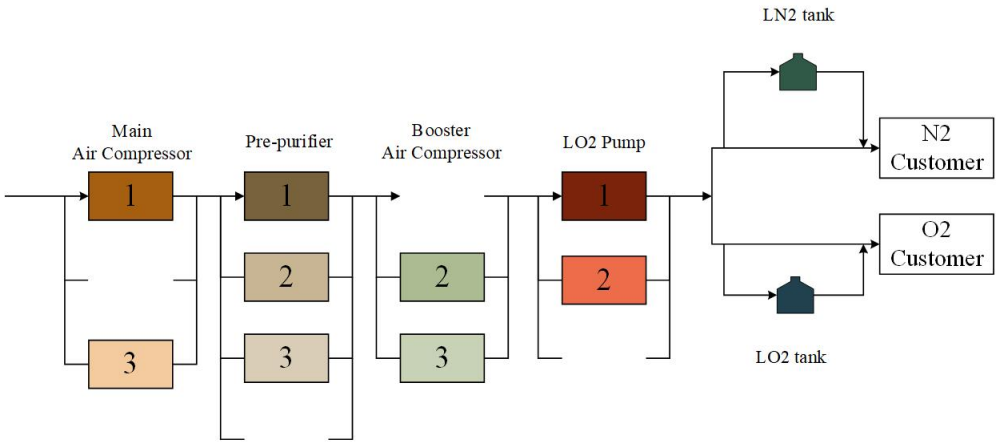

Figure 18: Optimal design when failure rates are doubled and repair rates are cut in half

First we perturb the parameters to make the units less reliable and harder to repair. For when the failure rates are doubled and the repair rates are cut in half, the optimal design is shown in Figure 18, where the only change comparing to the original design (Figure 17) is that the main air compressor switched one of the redundancies for a more expensive and more reliable one. And because of the changes in the reliability parameters, the expected LO2 penalty becomes \$181,769 , and the expected LN2 penalty becomes \$200,556 .

If the failure rates are multiplied by 5 and repair rates are divided by 5 (Figure 19), the best decision is to have the largest storage tanks (1500k gallon) for both products, and to have all the potential units in the compressor stages. The capital cost on the processing equipment is now \$8475k, while the capital cost on the storage tanks is \$1815k. The expected frequency of LO2 outage is 0.254 in the 10 year horizon, which incurs \$508,643 penalty. The expected frequency of LN2 outage is 0.391 in the 10 year horizon, which incurs \$781,340 penalty.

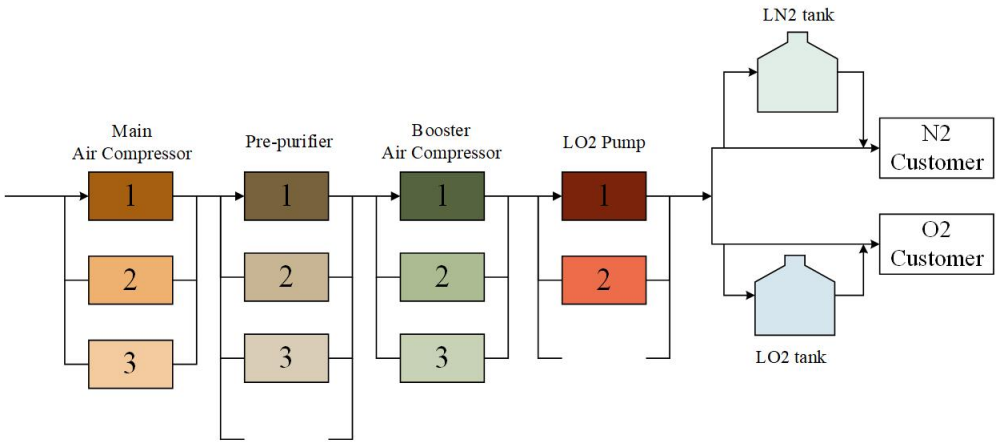

Figure 19: Optimal design when failure rates are multiplied by 5 and repair rates are divided by 5

Now we switch to the other direction where the failure rates are cut in half and the repair rates are doubled (Figure 20), and there is a huge improvement in the capital investment needed for the redundancies comparing to the nominal case ($3415k comparing to $6225k), but there has to be a raise on the storage side as a trade-off (1000k gallon for both LO2 and LN2 leading to $1186k capital cost). The expected frequency of LO2 outage is 0.237 in the 10 year horizon, which incurs $473,939 penalty. The expected frequency of LN2 outage is 0.295 in the 10 year horizon, which incurs $589,553 penalty.

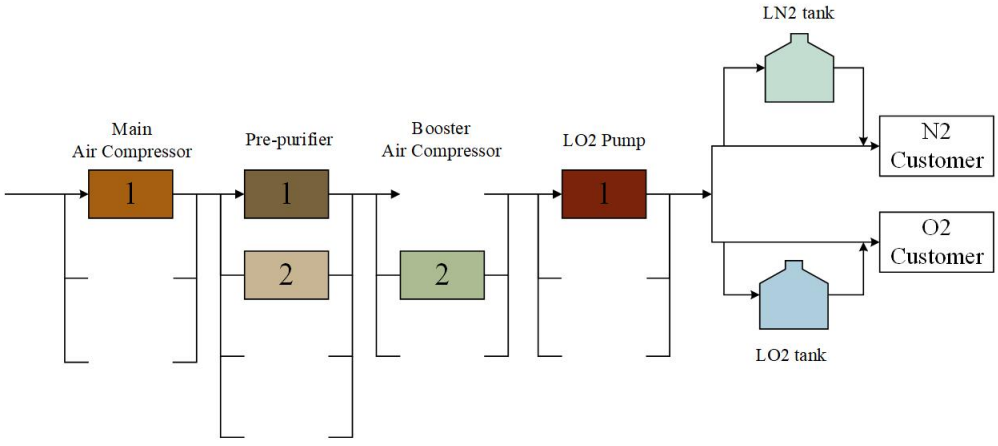

Figure 20: Optimal design when failure rates are cut in half and repair rates are doubled

Finally, when the units are assumed to be significantly more reliable than the nominal

case, the optimal design is to use the fewest number of redundancies and the smallest storage tanks. The investment on processing equipment is deemed to be \$3365k. 400k gallon tanks are chosen for both products, which lead to a \$452k cost. The expected frequency of LO2 outage is 0.0960 in the 10 year horizon, which incurs \$192,029 penalty. The expected frequency of LN2 outage is 0.125 in the 10 year horizon, which incurs \$249,535 penalty.

It can be seen from the last two cases that the optimizer chooses to pay more penalties rather than higher investment cost, as the opportunistic decrease of outage penalties are not enough to overcome capital commitment of installing more redundancies.

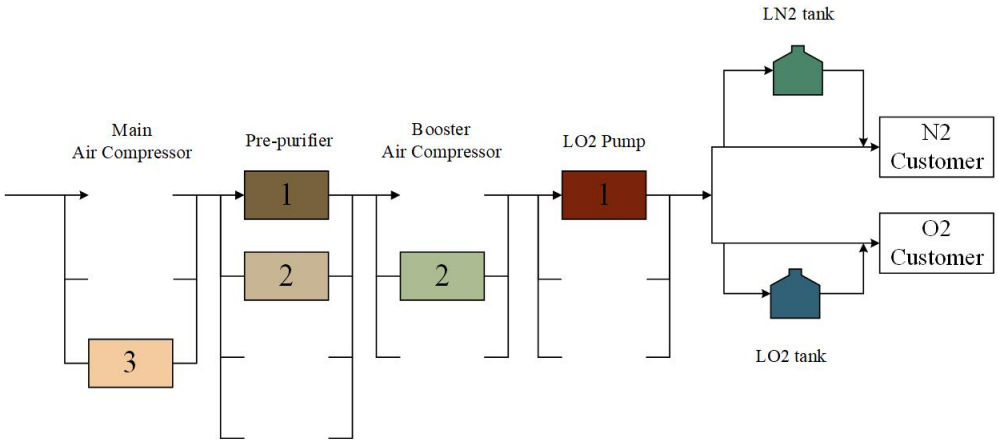

Figure 21: Optimal design when failure rates are divided by 5 and repair rates are multiplied by 5

Table 6 shows the numerical results and the computational statistics from both methods. It can be seen that the proposed game theoretic algorithm can solve the problem in much shorter time than the original MILP. Also, as the units become more reliable, the overall costs and penalties become lower.

Table 6: Numerical results and computational statistics of the sensitivity test cases

		Least reliable	Less reliable	More reliable	Most reliable
Objective value (K$)		11579.9	6722.4	5855.6	4258.5
Investment cost (K$)		8475	6235	3415	3365
LN2 penalty (K$)		508.6	181.8	666.8	192.1
LO2 penalty (K$)		781.3	200.6	587.8	249.4
The proposed algorithm	CPUs	9.2	2.6	2.3	2.3
	No. Iters	3	1	1	1
The original MILP (RST)	CPUs for parameters	2702.2	2828.6	2712.3	2721.1
	CPUs for models	1191.2	2198.2	604.6	189.1

8 Conclusion

In this paper, we addressed the optimization problem of reliable design for chemical processes, where design decisions are made regarding redundant equipment selection and storage tanks sizing. The aim is to minimize the total cost, which consists of the penalty from product unavailability and the cost of taking the reliability increasing measures, including having redundant units and storage tanks. An MILP model (RST) based on Markov Chain assumption is proposed and applied to the motivating example of an air separation unit, where the pipeline availability is essential for ensuring the continuation of downstream customer productions.

While the Markov Chain framework closely represents the stochastic process of equipment failures and repairs, and the filling and consumption of liquid storage, the state space representation leads to curse of dimensionality. To be able to tackle larger superstructures, we propose a game theoretic algorithm that decomposes and restructures the problem as a team game of the various processing stages, and arrives at a Nash Equilibrium among them. It is also shown that a good initial design that is close enough to the global optimum can be easily obtained for our problem, which guarantees the quality of the Nash Equilibrium

solution. A number of examples have been shown to illustrate the proposed algorithm's ability to solve to global optimality in orders of magnitude shorter time than the original MILP model (RST).

Nomenclature

Indices

k	The index of the processing stages
h	The index of single stage designs
$\bar{h}$	The index of the system designs
$\tilde{h}$	The index of the minus-one-stage system designs
s	The state index of single stages
$\bar{s}$	The state index of the system
$\tilde{s}$	The state index of the minus-one-stage systems
n	The index of storage tank size options

Parameters

$c\_unit_{k,h}$	The investment cost of design h in stage k
$W_{k,h}(s,s)$,$\boldsymbol{W}_{k,h}$	The transition rate (,matrix) of design h in stage k
$\pi_{k,h}(s)$,$\boldsymbol{\pi}_{k,h}$	The stationary probability distribution (,vector) of design h in stage k
$\sigma_{k,h}(s)$,$\boldsymbol{\sigma}_{k,h}$	The departing rate (,vector) of design h in stage k
$\bar{W}_{\bar{h}}(\bar{s},\bar{s})$,$\bar{\boldsymbol{W}}_{\bar{h}}$	The transition rate (,matrix) of system design $\bar{h}$
$\bar{\pi}_{\bar{h}}(\bar{s})$,$\bar{\boldsymbol{\pi}}_{\bar{h}}$	The stationary probability distribution (,vector) of system design $\bar{h}$
$\sigma_{\bar{h}}(\bar{s})$,$\bar{\boldsymbol{\sigma}}_{\bar{h}}$	The departing rate (,vector) of system design $\bar{h}$
$f_{\bar{h}}(\bar{s})$	The frequency of encountering state s of system design $\bar{h}$
T	Planned service time of the ASU
V_n^{LO2}	The reserve volume option n of liquid oxygen (tons)

V_n^{LN2} The reserve volume option n of liquid nitrogen (tons)

$c\_tank_n^{LO2}$ The investment cost of liquid oxygen tank of reserve volume V_n^{LO2}

$c\_tank_n^{LN2}$ The investment cost of liquid nitrogen tank of reserve volume V_n^{LN2}

δ^{LO2} Consumption rate of liquid oxygen (tons per day)

δ^{LN2} Consumption rate of liquid nitrogen (tons per day)

$penalty^{LO2}$ Penalty of liquid oxygen supply interruption (K$ per occurrence)

$penalty^{LN2}$ Penalty of liquid nitrogen supply interruption (K$ per occurrence)

$\hat{fr}_{n,\bar{h}}^{LO2}$ Over consumption frequency of liquid oxygen given that size n is selected for LO2 tank and $\bar{h}$ is selected for system design

$\hat{fr}_{n,\bar{h}}^{LN2}$ Over consumption frequency of liquid nitrogen given that size n is selected for LN2 tank and $\bar{h}$ is selected for system design

$\hat{FR}_{n,k,h(k,\bar{h})}^{LO2}$ The over consumption frequency of liquid oxygen that is due to the failure in stage k under system design $\bar{h}$, which corresponds to stage design h in stage k

$\hat{FR}_{n,k,h(k,\bar{h})}^{LN2}$ The over consumption frequency of liquid nitrogen that is due to the failure in stage k under system design $\bar{h}$, which corresponds to stage design h in stage k

$\hat{FR}_{n,k,h,\tilde{h}}^{LO2}$ The over consumption frequency of liquid oxygen that is due to the failure in stage k with design h and complementary design $\tilde{h}$

$\hat{FR}_{n,k,h(k,\bar{h})}^{LN2}$ The over consumption frequency of liquid nitrogen that is due to the failure in stage k with design h and complementary design $\tilde{h}$

Sets

K The index set of the processing stages

H_k The index set of the designs of stage k

$\bar{H}$ The index set of system designs

$\tilde{H}_k$ The index set of the complementary designs of stage k

N^{LO2} The index set of LO2 storage tank size options

N^{LN2} The index set of LN2 storage tank size options

$S_{k,h}$ The state space (set of all possible states) of design h in stage k

$S^f_{k,h}$ The set of all failure states of design h in stage k

$\bar{S}_{\bar{h}}$ The state space of the system design $\bar{h}$

$\bar{S}^f_{\bar{h}}$ The set of all failure states of system design $\bar{h}$

$\tilde{S}_{k,\tilde{h}}$ The state space of the complementary design $\tilde{h}$ of stage k

Variables

$z_{k,h}$ Binary variable that indicates the selection of design h for stage k

x^{LO2}_n Binary variable that indicates the selection of tank size option n for liquid oxygen

x^{LN2}_n Binary variable that indicates the selection of tank size option n for liquid nitrogen

$rt_{\bar{h}}(\bar{s})$ Random variable of the residence time of state $\bar{s}$ of system design $\bar{h}$

$V^{LO2dec}_{\bar{h}}(\bar{s})$ Random variable of the volume of liquid oxygen decreasing during failure state $\bar{s}$

$V^{LN2dec}_{\bar{h}}(\bar{s})$ Random variable of the volume of liquid nitrogen decreasing during failure state $\bar{s}$

$fr^{LO2}_{n,\bar{h}}$ Over consumption frequency of liquid oxygen given that size n is selected for LO2 tank and $\bar{h}$ is selected for system design

$fr^{LN2}_{n,\bar{h}}$ Over consumption frequency of liquid nitrogen given that size n is selected for LN2 tank and $\bar{h}$ is selected for system design

C^U Investment cost on processing units

C^T Investment cost on storage tanks

PN Expected penalty from supply interruptions

Acknowledgement

The authors thank the support from National Science Foundation under grant CBET-1705372, Praxair, Inc. (Now Linde plc), and Center for Advanced Process Decision-making at Carnegie Mellon University.

Appendix A Relationship between the system level quantities and the stage level quantities

In this appendix, we show how to obtain the system level quantities, $\bar{\boldsymbol{\pi}}$, and $\bar{\boldsymbol{\sigma}}$, through the Kronecker products of the stage level quantities (where of each stage n they are denoted as $\boldsymbol{\pi}_n$, and $\boldsymbol{\sigma}_n$).

Suppose $\boldsymbol{Q}^1_{m\times m}$ is the transition matrix based on certain design of stage 1, $\boldsymbol{Q}^2_{n\times n}$ is the transition matrix based on certain design of stage 2, and $\boldsymbol{Q}_{mn\times mn}$ is the transition matrix based on the corresponding system design. By definition, we have,

$$\boldsymbol{Q}_{mn\times mn} = \boldsymbol{I}_{n\times n} \otimes \boldsymbol{Q}^1_{m\times m} + \boldsymbol{Q}^2_{n\times n} \otimes \boldsymbol{I}_{m\times m} \tag{A.50}$$

Let $\boldsymbol{\pi}_m$, $\boldsymbol{\pi}_n$, and $\bar{\boldsymbol{\pi}}_{mn}$ be the corresponding stationary probability vectors, then they satisfy (A.51), (A.52) and (A.53) respectively:

$$\boldsymbol{\pi}^T_m \boldsymbol{Q}^1_{m\times m} = \mathbf{0}^T_m \tag{A.51}$$

$$\boldsymbol{\pi}^T_n \boldsymbol{Q}^2_{n\times n} = \mathbf{0}^T_n \tag{A.52}$$

$$\bar{\boldsymbol{\pi}}^T_{mn} \boldsymbol{Q}_{mn\times mn} = \mathbf{0}^T_{mn\times mn} \tag{A.53}$$

Let $\boldsymbol{\sigma}_m$, $\boldsymbol{\sigma}_n$, and $\bar{\boldsymbol{\sigma}}_{mn}$ be the corresponding diagonal vectors as defined in (A.54), (A.55),

and (A.56).

$$\boldsymbol{\sigma}_m = diag(\boldsymbol{Q}^1_{m\times m}) \tag{A.54}$$

$$\boldsymbol{\sigma}_n = diag(\boldsymbol{Q}^2_{n\times n}) \tag{A.55}$$

$$\bar{\boldsymbol{\sigma}}_{mn} = diag(\boldsymbol{Q}_{mn\times mn}) \tag{A.56}$$

It then follows that,

$$\bar{\boldsymbol{\sigma}}_{mn} = \mathbf{1}_n \otimes \boldsymbol{\sigma}_m + \boldsymbol{\sigma}_n \otimes \mathbf{1}_m \tag{A.57}$$

Next we show that

$$\bar{\boldsymbol{\pi}}_{mn} = \boldsymbol{\pi}_n \otimes \boldsymbol{\pi}_m \tag{A.58}$$

From (A.51) and (A.52) we have

$$(\boldsymbol{\pi}_n \otimes \boldsymbol{\pi}_m)^T (\boldsymbol{I}_{n\times n} \otimes \boldsymbol{Q}^1_{m\times m}) \tag{A.59}$$

$$=(\pi_n(1)\boldsymbol{\pi}_m^T, \pi_n(2)\boldsymbol{\pi}_m^T, ..., \pi_n(n)\boldsymbol{\pi}_m^T) \begin{pmatrix} \boldsymbol{Q}^1_{m\times m} & & & \\ & \boldsymbol{Q}^1_{m\times m} & & \\ & & \ddots & \\ & & & \boldsymbol{Q}^1_{m\times m} \end{pmatrix} = \mathbf{0}^T_{mn\times mn} \tag{A.60}$$

$$(\boldsymbol{\pi}_n \otimes \boldsymbol{\pi}_m)^T (\boldsymbol{Q}^2_{n\times n} \otimes \boldsymbol{I}_{m\times m}) \tag{A.61}$$

$$= (\pi_n(1)\boldsymbol{\pi}_m^T, \pi_n(2)\boldsymbol{\pi}_m^T, ..., \pi_n(n)\boldsymbol{\pi}_m^T) \begin{pmatrix} Q^2_{n\times n}(1,1)I_{m\times m} & Q^2_{n\times n}(1,2)I_{m\times m} & \cdots & Q^2_{n\times n}(1,n)I_{m\times m} \\ \vdots & \vdots & \ddots & \vdots \\ Q^2_{n\times n}(n,1)I_{m\times m} & Q^2_{n\times n}(n,2)I_{m\times m} & \cdots & Q^2_{n\times n}(n,n)I_{m\times m} \end{pmatrix} \tag{A.62}$$

$$= \mathbf{0}^T_{mn\times mn} \tag{A.63}$$

Therefore,

$$\bar{\boldsymbol{\pi}}^T_{mn} \boldsymbol{Q}_{mn\times mn} \tag{A.64}$$

$$= (\boldsymbol{\pi}_n \otimes \boldsymbol{\pi}_m)^T \boldsymbol{Q}_{mn\times mn} \tag{A.65}$$

$$= (\boldsymbol{\pi}_n \otimes \boldsymbol{\pi}_m)^T (\boldsymbol{I}_{n\times n} \otimes \boldsymbol{Q}^1_{m\times m} + \boldsymbol{Q}^2_{n\times n} \otimes \boldsymbol{I}_{m\times m}) \tag{A.66}$$

$$= \mathbf{0}^T_{mn\times mn} \tag{A.67}$$

Appendix B Approximation of the outage frequency parameters

In this appendix, we show how the complicating parameters, $\hat{fr}^{LO2}_{n,\bar{h}}$ and $\hat{fr}^{LN2}_{n,\bar{h}}$, can be approximated by stage-wise decomposition, and under the assumptions that the single unit failure rates are of $O(10^{-4})$, and the single unit repair rates are of $O(10^{-2})$.

The expression of $\hat{fr}^{LO2}_{n,\bar{h}}$ is as shown in equation B.1.

$$\hat{fr}^{LO2}_{n,\bar{h}} = \sum_{\bar{s}\in\bar{S}^f_{\bar{h}}} \bar{\pi}_{\bar{h}}(\bar{s}) \cdot \bar{\sigma}_{\bar{h}}(\bar{s}) \cdot e^{-\frac{V^{LO2}_n}{\delta^{LO2}}\bar{\sigma}_{\bar{h}}(\bar{s})} \tag{B.1}$$

Without loss of generality, we drop the indices of all the V and δ and look into the following

expression (B.2):

$$A(\bar{h}) = \sum_{\bar{s} \in \bar{S}^f_{\bar{h}}} \bar{\pi}_{\bar{h}}(\bar{s}) \cdot \bar{\sigma}_{\bar{h}}(\bar{s}) \cdot e^{-\frac{V}{\delta}\bar{\sigma}_{\bar{h}}(\bar{s})} \tag{B.2}$$

According to equations (7) and (8), (B.2) can be expanded as shown in (B.3).

$$A(\bar{h}) = \sum_{\bar{s} \in \bar{S}^f_{\bar{h}}} [\sum_{k \in K} \sigma_{k,h(k,\bar{h})}(s(k,\bar{s}))][\prod_{k \in K} \pi_{k,h(k,\bar{h})}(s(k,\bar{s})) \cdot e^{-\frac{V}{\delta}\sigma_{k,h(k,\bar{h})}(s(k,\bar{s}))}] \tag{B.3}$$

From (B.3) to (B.4), $\bar{S}^f_{\bar{h}}$, the set of system failure states, breaks down into $|K|$ disjoint subsets, $\bar{S}^f_{k,h(k,\bar{h})}$, based on which stage the failure actually happens.

$$\begin{aligned} A(\bar{h}) =& \sum_{k \in K} \sum_{\bar{s} \in \bar{S}^f_{k,h(k,\bar{h})}} [\sum_{k \in K} \sigma_{k,h(k,\bar{h})}(s(k,\bar{s}))][\prod_{k \in K} \pi_{k,h(k,\bar{h})}(s(k,\bar{s})) \cdot e^{-\frac{V}{\delta}\sigma_{k,h(k,\bar{h})}(s(k,\bar{s}))}] \\ =& \sum_{k \in K} \sum_{\bar{s} \in \bar{S}^f_{k,h(k,\bar{h})}} \{[\sigma_{k,h(k,\bar{h})}(s(k,\bar{s})) + \sum_{l \in K, l \neq k} \sigma_{l,h(l,\bar{h})}(s(l,\bar{s}))] \cdot \\ & [\pi_{k,h(k,\bar{h})}(s(k,\bar{s})) \cdot e^{-\frac{V}{\delta}\sigma_{k,h(k,\bar{h})}(s(k,\bar{s}))} \cdot \prod_{l \in K, l \neq k} \pi_{l,h(l,\bar{h})}(s(l,\bar{s})) \cdot e^{-\frac{V}{\delta}\sigma_{l,h(l,\bar{h})}(s(l,\bar{s}))}]\} \end{aligned} \tag{B.4}$$

For each stage k, we let $\tilde{h}$ index the potential designs of the complementary subsystem obtained by subtracting stage k from the entire system. For example, when dealing with stage 1, the complementary subsystem refers to the system consists of stages 2, 3, and 4. $\tilde{h}(k,\bar{h})$ is the index of the potential complementary design of stage k that is part of system design $\bar{h}$. Following the idea of (7) and (8), the summations and products over $l \in K, l \neq k$ can be folded into the corresponding quantities of the complementary designs as shown in

(B.5).

$$A(\bar{h}) = \sum_{k\in K} \sum_{\bar{s}\in \bar{S}^f_{k,h(k,\bar{h})}} \{[\sigma_{k,h(k,\bar{h})}(s(k,\bar{s})) + \tilde{\sigma}_{k,\tilde{h}(k,\bar{h})}(\tilde{s}(l,\bar{s}))] \cdot [\pi_{k,h(k,\bar{h})}(s(k,\bar{s})) \cdot e^{-\frac{V}{\delta}\sigma_{k,h(k,\bar{h})}(s(k,\bar{s}))} \cdot \tilde{\pi}_{k,\tilde{h}(k,\bar{h})}(\tilde{s}(l,\bar{s})) \cdot e^{-\frac{V}{\delta}\tilde{\sigma}_{k,\tilde{h}(k,\bar{h})}(\tilde{s}(l,\bar{s}))}]\} \quad \text{(B.5)}$$

Moreover, since the set of system states with failure in stage k, $\bar{S}^f_{k,h(k,\bar{h})}$, is the Cartesian product of the set of failure stage states of stage k, $S^f_{k,h(k,\bar{h})}$, and the set of non-failure (working) states of its complementary sub-system, $\tilde{S}^w_{k,\tilde{h}(k,\bar{h})}$, therefore, $A(\bar{h})$ can be further rewritten as in (B.6) and then (B.7).

$$\begin{aligned} A(\bar{h}) =& \sum_{k\in K} \sum_{s\in S^f_{k,h(k,\bar{h})}} \sum_{\tilde{s}\in \tilde{S}^w_{k,\tilde{h}(k,\bar{h})}} \{[\sigma_{k,h(k,\bar{h})}(s) + \tilde{\sigma}_{k,\tilde{h}(k,\bar{h})}(\tilde{s})] \\ & \cdot [\pi_{k,h(k,\bar{h})}(s) \cdot e^{-\frac{V}{\delta}\sigma_{k,h(k,\bar{h})}(s)} \cdot \tilde{\pi}_{k,\tilde{h}(k,\bar{h})}(\tilde{s}) \cdot e^{-\frac{V}{\delta}\tilde{\sigma}_{k,\tilde{h}(k,\bar{h})}(\tilde{s})}]\} \quad \text{(B.6)} \\ =& \sum_{k\in K} \sum_{s\in S^f_{k,h(k,\bar{h})}} [\pi_{k,h(k,\bar{h})}(s) \cdot e^{-\frac{V}{\delta}\sigma_{k,h(k,\bar{h})}(s)} \cdot \sigma_{k,h(k,\bar{h})}(s) \\ & \cdot \sum_{\tilde{s}\in \tilde{S}^w_{k,\tilde{h}(k,\bar{h})}} \tilde{\pi}_{k,\tilde{h}(k,\bar{h})}(\tilde{s}) \cdot e^{-\frac{V}{\delta}\tilde{\sigma}_{k,\tilde{h}(k,\bar{h})}(\tilde{s})} \cdot (1 + \frac{\tilde{\sigma}_{k,\tilde{h}(k,\bar{h})}(\tilde{s})}{\sigma_{k,h(k,\bar{h})}(s)})] \quad \text{(B.7)} \end{aligned}$$

We let

$$\sum_{\tilde{s}\in \tilde{S}^w_{k,\tilde{h}(k,\bar{h})}} \tilde{\pi}_{k,\tilde{h}(k,\bar{h})}(\tilde{s}) \cdot e^{-\frac{V}{\delta}\tilde{\sigma}_{k,\tilde{h}(k,\bar{h})}(\tilde{s})} \cdot (1 + \frac{\tilde{\sigma}_{k,\tilde{h}(k,\bar{h})}(\tilde{s})}{\sigma_{k,h(k,\bar{h})}(s)}) = B_{k,\tilde{h}(k,\bar{h})}(s) + E_{k,\tilde{h}(k,\bar{h})}(s), \quad \text{(B.8)}$$

where

$$B_{k,\tilde{h}(k,\bar{h})}(s) = \tilde{\pi}_{k,\tilde{h}(k,\bar{h})}(1) \cdot e^{-\frac{V}{\delta}\sigma_{k,\tilde{h}(k,\bar{h})}(1)} \cdot (1 + \frac{\tilde{\sigma}_{k,\tilde{h}(k,\bar{h})}(1)}{\sigma_{k,h(k,\bar{h})}(s)}), \quad \text{(B.9)}$$

and

$$E_{k,\tilde{h}(k,\bar{h})}(s) = \sum_{\tilde{s}\in\tilde{S}^{w}_{k,\tilde{h}(k,\bar{h})}\setminus\{1\}} \tilde{\pi}_{k,\tilde{h}(k,\bar{h})}(\tilde{s}) \cdot e^{-\frac{V}{\delta}\tilde{\sigma}_{k,\tilde{h}(k,\bar{h})}(\tilde{s})} \cdot (1 + \frac{\tilde{\sigma}_{k,\tilde{h}(k,\bar{h})}(\tilde{s})}{\sigma_{k,h(k,\bar{h})}(s)}), \tag{B.10}$$

where state ($\tilde{s} = 1$) refers to the all-good state of the sub-system $k, \tilde{h}$. With (B.7) and (B.8), we have,

$$A(\bar{h}) = \sum_{k\in K} \sum_{s\in S^{f}_{k,h(k,\bar{h})}} \pi_{k,h(k,\bar{h})}(s) \cdot e^{-\frac{V}{\delta}\sigma_{k,h(k,\bar{h})}(s)} \cdot \sigma_{k,h(k,\bar{h})}(s) \cdot (B_{k,\tilde{h}(k,\bar{h})}(s) + E_{k,\tilde{h}(k,\bar{h})}(s)). \tag{B.11}$$

$\sigma_{k,\tilde{h}(k,\bar{h})}(1)$ is the sum of the failure rates of all the failure modes of the first unit selected for stage k, therefore, $\sigma_{k,\tilde{h}(k,\bar{h})}(1) \sim O(10^{-4})$. Since state s here only include the failure states of each stage, there is at least one repair rate contributing to $\sigma_{k,h(k,\bar{h})}(s)$, so $\sigma_{k,h(k,\bar{h})}(s) \sim O(10^{-2})$. $\frac{V}{\delta}$ ranges from $O(10)$ to $O(10^2)$. Based on the value and order estimations stated above, we can estimate the value of $B_{k,\tilde{h}(k,\bar{h})}(s)$ in (B.12).

$$\begin{aligned} B_{k,\tilde{h}(k,\bar{h})}(s) &= \tilde{\pi}_{k,\tilde{h}(k,\bar{h})}(1) \cdot (1 - \frac{V}{\delta}\tilde{\sigma}_{k,\tilde{h}(k,\bar{h})}(1)) \cdot (1 + O(10^{-2})) \\ &= \tilde{\pi}_{k,\tilde{h}(k,\bar{h})}(1) \cdot (1 - O(10^{-2})) \cdot (1 + O(10^{-2})) = \tilde{\pi}_{k,\tilde{h}(k,\bar{h})}(1) \cdot (1 \pm O(10^{-2})). \end{aligned} \tag{B.12}$$

For the second term, $E_{k,\tilde{h}(k,\bar{h})}(s)$, Let it be written as shown in (B.13).

$$E_{k,\tilde{h}(k,\bar{h})}(s) = \sum_{\tilde{s}\in\tilde{S}^{w}_{k,\tilde{h}(k,\bar{h})}\setminus\{1\}} \tilde{\pi}_{k,\tilde{h}(k,\bar{h})}(\tilde{s}) \cdot G_{k,\tilde{h}(k,\bar{h})}(s,\tilde{s}) \tag{B.13}$$

We examine the derivative of $G_{k,\tilde{h}(k,\bar{h})}(s,\tilde{s})$ with regard to $\tilde{\sigma}_{k,\tilde{h}(k,\bar{h})}(\tilde{s})$.

$$\frac{dG_{k,\tilde{h}(k,\bar{h})}(s,\tilde{s})}{d\tilde{\sigma}_{k,\tilde{h}(k,\bar{h})}(\tilde{s})} = \frac{d}{d\tilde{\sigma}_{k,\tilde{h}(k,\bar{h})}(\tilde{s})}(e^{-\frac{V}{\delta}\tilde{\sigma}_{k,\tilde{h}(k,\bar{h})}(\tilde{s})} \cdot (1 + \frac{\tilde{\sigma}_{k,\tilde{h}(k,\bar{h})}(\tilde{s})}{\sigma_{k,h(k,\bar{h})}(s)})) \tag{B.14}$$

$$= e^{-\frac{V}{\delta}\tilde{\sigma}_{k,\tilde{h}(k,\bar{h})}(\tilde{s})}(-\frac{V}{\delta\cdot\sigma_{k,h(k,\bar{h})}(s)}\tilde{\sigma}_{k,\tilde{h}(k,\bar{h})}(\tilde{s})+\frac{V}{\delta}-\frac{1}{\sigma_{k,h(k,\bar{h})}(s)}) : \begin{cases} > 0, & \text{if } \tilde{\sigma}_{k,\tilde{h}(k,\bar{h})}(\tilde{s}) \leq \frac{\delta}{V} - \sigma_{k,h(k,\bar{h})}(s) \\ \leq 0, & \text{if } \tilde{\sigma}_{k,\tilde{h}(k,\bar{h})}(\tilde{s}) > \frac{\delta}{V} - \sigma_{k,h(k,\bar{h})}(s) \end{cases} \tag{B.15}$$

By definition, $\tilde{\sigma}_{k,\tilde{h}(k,\bar{h})}(\tilde{s})$ is always positive, therefore, we are only concerned about the value on the positive side.

$$\max_{\tilde{\sigma}_{k,\tilde{h}(k,\bar{h})}(\tilde{s})>0} \quad G_{k,\tilde{h}(k,\bar{h})}(s,\tilde{s}) \quad = \begin{cases} 1 & , \frac{\delta}{V} \leq \sigma_{k,h(k,\bar{h})}(s) \\ \frac{\delta}{V\cdot\sigma_{k,h(k,\bar{h})}(s)} \cdot e^{\frac{V}{\delta}\sigma_{k,h(k,\bar{h})}(s)-1} & , \frac{\delta}{V} > \sigma_{k,h(k,\bar{h})}(s) \end{cases} \tag{B.16}$$

With certain δ and $\sigma_{k,h(k,\bar{h})}(s)$ ($\sim O(10^{-2})$), $\frac{\delta}{V\cdot\sigma_{k,h(k,\bar{h})}(s)} \cdot e^{\frac{V}{\delta}\sigma_{k,h(k,\bar{h})}(s)-1}$ achieves its maximum at the smallest possible tank size V, where $\frac{\delta}{V} \sim O(10^{-1})$, and $\frac{\delta}{V\cdot\sigma_{k,h(k,\bar{h})}(s)} \cdot e^{\frac{V}{\delta}\sigma_{k,h(k,\bar{h})}(s)-1} \sim O(1)$. Based on the above order of magnitude estimations, we have,

$$E_{k,\tilde{h}(k,\bar{h})}(s) \leq (1-\tilde{\pi}_{k,\tilde{h}(k,\bar{h})}(1)) \cdot O(1) \tag{B.17}$$

State ($\tilde{s}=1$) refers to the all-good state of the sub-system $k,\tilde{h}$, therefore, $\tilde{\pi}_{k,\tilde{h}(k,\bar{h})}(1) = 1-O(10^{-2})$. Therefore,

$$B_{k,\tilde{h}(k,\bar{h})}(s) + E_{k,\tilde{h}(k,\bar{h})}(s) = (1-O(10^{-2}))(1\pm O(10^{-2})) + O(10^{-2}) = 1 \pm O(10^{-2}) \tag{B.18}$$

$$A(\bar{h}) = \sum_{k\in K} \sum_{s\in S^f_{k,h(k,\bar{h})}} \pi_{k,h(k,\bar{h})}(s) \cdot e^{-\frac{V}{\delta}\sigma_{k,h(k,\bar{h})}(s)} \cdot \sigma_{k,h(k,\bar{h})}(s) \cdot (1 \pm O(10^{-2})) \tag{B.19}$$

$$\hat{fr}^{LO2}_{n,\bar{h}} = \sum_{k\in K} \sum_{s\in S^f_{k,h(k,\bar{h})}} \pi_{k,h(k,\bar{h})}(s) \cdot e^{-\frac{V^{LO2}_n}{\delta^{LO2}}\sigma_{k,h(k,\bar{h})}(s)} \cdot \sigma_{k,h(k,\bar{h})}(s) \cdot (1 \pm O(10^{-2})) \tag{B.20}$$

Appendix C The objective function sensitivity of (IDS) to parameters $\hat{FR}^{LO2}_{n,k,h}$ and $\hat{FR}^{LN2}_{n,k,h}$

In this appendix we derive the upper bounds of the objective function sensitivity of the independent design selection problem (IDS) to the complicating parameters $\hat{FR}^{LO2}_{n,k,h}$ and $\hat{FR}^{LN2}_{n,k,h}$, in order to show that the initial design obtained from approximated parameters are close enough to the global optimum.

First we write down the general form of the MILP as follows, where x are the binary variables, and y are the continuous variables. $\hat{FR}^{LO2}_{n,k,h}$ and $\hat{FR}^{LN2}_{n,k,h}$ are part of A and c, which are approximated with $\Theta^{LO2}_{n,k,h}$ and $\Theta^{LO2}_{n,k,h}$ at the initialization phase of the proposed game-theoretic algorithm.

$$\min \quad gx + hy \tag{C.1}$$

$$\text{s.t.} \quad Ax + By \leq c \tag{C.2}$$

$$Dx \leq e \tag{C.3}$$

$$x \in \{0,1\}^n \tag{C.4}$$

$$y \in R^m_+ \tag{C.5}$$

Let (x^o, y^o) be the solution to the problem where the parameters of concern are equal to our initial approximation in the paper:

$$(x^o, y^o) = \arg\min\{gx + hy | A^o x + By \leq c^o, Dx \leq e, x \in \{0,1\}^n, y \in R^m_+\} \tag{C.6}$$

Let (x^*, y^*) be the solution to the problem where the parameters of concern are equal to those calculated from the global optimal solution. In other words, the problem can be viewed as an equilibrium checking problem for the global optimal strategy, which is also a

Nash equilibrium strategy.

$$(x^*, y^*) = \arg\min\{gx + hy | A^*x + By \leq c^*, Dx \leq e, x \in \{0,1\}^n, y \in R_+^m\} \tag{C.7}$$

By definition of optimality, As shown in (C.8), by the definition of optimality, if we specify the binary variable values in the initial problem (C.6) withx^*, the optimization result is greater than the overall optimum of that problem.

$$gx^o + hy^o \leq gx^* + \min\{hy | By \leq c^o - A^o x^*, y \in R_+^m\} \tag{C.8}$$

Our major concern is the difference between the optimal objective value, $(gx^* + hy^*)$ and the objective value of the approximated solution, $(gx^o + \min\{hy | By \leq c' - A'x^o, y \in R_+^m\})$, where in A' and c', the parameters of concern are calculated from the approximated strategy x^o. With (C.8), we can bound the difference with (C.9), where the problem becomes the objective value sensitivity to RHS of the LP from fixing the binary variables $(x = x^o)$.

$$\begin{aligned} Err =& (gx^o + \min\{hy | By \leq c' - A'x^o, y \in R_+^m\}) - (gx^* + hy^*) \\ \leq& (\min\{hy | By \leq c^o - A^o x^*, y \in R_+^m\} - hy^*) + (\min\{hy | By \leq c' - A'x^o, y \in R_+^m\} - hy^o) \end{aligned} \tag{C.9}$$

$$\begin{aligned} =& (\min\{hy | By \leq c^o - A^o x^*, y \in R_+^m\} - \min\{hy | By \leq c^* - A^* x^*, y \in R_+^m\}) \\ &+ (\min\{hy | By \leq c' - A'x^o, y \in R_+^m\} - \min\{hy | By \leq c^o - A^o x^o, y \in R_+^m\}) \end{aligned} \tag{C.10}$$

For model (IDS), the LP from fixing the discrete variables ($x = x^*$) reduces to the following,

$$\min \quad T(penalty^{LO2} \cdot \sum_{n \in N^{LO2}} \sum_{k \in K} \sum_{h \in H_k} fr^{LO2}_{n,k,h} + penalty^{LN2} \cdot \sum_{n \in N^{LO2}} \sum_{k \in K} \sum_{h \in H_k} fr^{LN2}_{n,k,h}) \tag{C.11}$$

$$\text{s.t.} \quad fr^{LO2}_{n,k,h} \leq \hat{FR}^{LO2}_{n,k,h}, \quad \forall (x^{LO2}_n)^* = 1, k \in K, h \in H_k \tag{C.12}$$

$$fr^{LO2}_{n,k,h} \leq \hat{FR}^{LO2}_{n,k,h}, \quad \forall (z_{k,h})^* = 1, n \in N^{LO2} \tag{C.13}$$

$$-fr^{LO2}_{n,k,h} \leq -\hat{FR}^{LO2}_{n,k,h}, \quad \forall (z_{k,h})^* = 1, (x^{LO2}_n)^* = 1 \tag{C.14}$$

$$fr^{LO2}_{n,k,h} \leq 0, \quad \forall (x^{LO2}_n)^* = 0, k \in K, h \in H_k \tag{C.15}$$

$$fr^{LO2}_{n,k,h} \leq 0, \quad \forall (z_{k,h})^* = 0, n \in N^{LO2} \tag{C.16}$$

$$-fr^{LO2}_{n,k,h} \leq \hat{FR}^{LO2}_{n,k,h}, \quad \forall (z_{k,h})^* = 0, (x^{LO2}_n)^* = 0 \tag{C.17}$$

$$-fr^{LO2}_{n,k,h} \leq 0, \quad \forall (z_{k,h})^* = 0, (x^{LO2}_n)^* = 1 \text{ OR } (z_{k,h})^* = 1, (x^{LO2}_n)^* = 0 \tag{C.18}$$

$$fr^{LN2}_{n,k,h} \leq \hat{FR}^{LN2}_{n,k,h}, \quad \forall (x^{LN2}_n)^* = 1, k \in K, h \in H_k \tag{C.19}$$

$$fr^{LN2}_{n,k,h} \leq \hat{FR}^{LN2}_{n,k,h}, \quad \forall (z_{k,h})^* = 1, n \in N^{LN2} \tag{C.20}$$

$$-fr^{LN2}_{n,k,h} \leq -\hat{FR}^{LN2}_{n,k,h}, \quad \forall (z_{k,h})^* = 1, (x^{LN2}_n)^* = 1 \tag{C.21}$$

$$fr^{LN2}_{n,k,h} \leq 0, \quad \forall (x^{LN2}_n)^* = 0, k \in K, h \in H_k \tag{C.22}$$

$$fr^{LN2}_{n,k,h} \leq 0, \quad \forall (z_{k,h})^* = 0, n \in N^{LN2} \tag{C.23}$$

$$-fr^{LN2}_{n,k,h} \leq \hat{FR}^{LN2}_{n,k,h}, \quad \forall (z_{k,h})^* = 0, (x^{LN2}_n)^* = 0 \tag{C.24}$$

$$-fr^{LN2}_{n,k,h} \leq 0, \quad \forall (z_{k,h})^* = 0, (x^{LN2}_n)^* = 1 \text{ OR } (z_{k,h})^* = 1, (x^{LN2}_n)^* = 0 \tag{C.25}$$

At the optimal point,

$$\begin{aligned}
&\min\{hy|By \leq c^o - A^o x^*, y \in R_+^m\} \\
=&T(penalty^{LO2} \cdot \sum_{k\in K} (\hat{FR}^{LO2}_{n,k,h,\text{ s.t. } (z_{k,h})^*=1,(x_n^{LO2})^*=1})^o + penalty^{LN2} \cdot \sum_{k\in K} (\hat{FR}^{LN2}_{n,k,h,\text{ s.t. } (z_{k,h})^*=1,(x_n^{LN2})^*=1})^o
\end{aligned} \tag{C.26}$$

We can obtain similar expressions for the other terms in (C.10). Based on (40) and (C.8), there is

$$\begin{aligned}
Err \leq& O(10^{-2}) \cdot T \cdot [penalty^{LO2} \cdot \sum_{k\in K} (\hat{FR}^{LO2}_{n,k,h,\text{ s.t. } (z_{k,h})^*=1,(x_n^{LO2})^*=1})^* \\
&+ penalty^{LN2} \cdot \sum_{k\in K} (\hat{FR}^{LN2}_{n,k,h,\text{ s.t. } (z_{k,h})^*=1,(x_n^{LN2})^*=1})^*] \\
&+ O(10^{-2}) \cdot T \cdot [penalty^{LO2} \cdot \sum_{k\in K} (\hat{FR}^{LO2}_{n,k,h,\text{ s.t. } (z_{k,h})^o=1,(x_n^{LO2})^o=1})^o \\
&+ penalty^{LN2} \cdot \sum_{k\in K} (\hat{FR}^{LN2}_{n,k,h,\text{ s.t. } (z_{k,h})^o=1,(x_n^{LN2})^o=1})^o] \qquad \text{(C.27)} \\
=& O(10^{-2}) \cdot (hy^* + hy^o) \qquad \text{(C.28)} \\
\leq& O(10^{-2}) \cdot (hy^* + gx^* + hy^* \cdot (1 + O(10^{-2}))) \qquad \text{(C.29)}
\end{aligned}$$

References

(1) Achkar, V. G., Cafaro, V. G., Mendez, C. A., and Cafaro, D. C. (2019). Discrete-time milp formulation for the optimal scheduling of maintenance tasks on oil and gas production assets. *Industrial & Engineering Chemistry Research*.

(2) Aguilar, O., Kim, J.-K., Perry, S., and Smith, R. (2008). Availability and reliability considerations in the design and optimisation of flexible utility systems. *Chemical Engineering Science*, 63(14):3569–3584.

(3) Amaran, S., Zhang, T., Sahinidis, N. V., Sharda, B., and Bury, S. J. (2016). Medium-

term maintenance turnaround planning under uncertainty for integrated chemical sites. *Computers & Chemical Engineering*, 84:422–433.

(4) Castillo, L. and Dorao, C. A. (2012). Consensual decision-making model based on game theory for lng processes. *Energy conversion and management*, 64:387–396.

(5) Cheung, K.-Y., Hui, C.-W., Sakamoto, H., Hirata, K., and O'Young, L. (2004). Short-term site-wide maintenance scheduling. *Computers & chemical engineering*, 28(1):91–102.

(6) Gong, J. and You, F. (2018). Resilient design and operations of process systems: Nonlinear adaptive robust optimization model and algorithm for resilience analysis and enhancement. *Computers & Chemical Engineering*, 116:231–252.

(7) Kuo, W. and Wan, R. (2007). Recent advances in optimal reliability allocation. In *Computational intelligence in reliability engineering*, pages 1–36. Springer.

(8) Lou, H. H., Kulkarni, M., Singh, A., and Huang, Y. L. (2004). A game theory based approach for emergy analysis of industrial ecosystem under uncertainty. *Clean Technologies and Environmental Policy*, 6(3):156–161.

(9) Pistikopoulos, E. N., Vassiliadis, C. G., Arvela, J., and Papageorgiou, L. G. (2001). Interactions of maintenance and production planning for multipurpose process plants a system effectiveness approach. *Industrial & engineering chemistry research*, 40(14):3195–3207.

(10) Sericola, B. (2013). *Markov Chains: Theory and Applications*. John Wiley & Sons.

(11) Tan, J. S. and Kramer, M. A. (1997). A general framework for preventive maintenance optimization in chemical process operations. *Computers & Chemical Engineering*, 21(12):1451–1469.

(12) Terrazas-Moreno, S., Grossmann, I. E., Wassick, J. M., and Bury, S. J. (2010). Optimal design of reliable integrated chemical production sites. *Computers & Chemical Engineering*, 34(12):1919–1936.

(13) Thomaidis, T. and Pistikopoulos, E. (1994). Integration of flexibility, reliability and maintenance in process synthesis and design. *Computers & Chemical Engineering*, 18:S259–S263.

(14) Thomaidis, T. V. and Pistikopoulos, E. (1995). Optimal design of flexible and reliable process systems. *IEEE transactions on reliability*, 44(2):243–250.

(15) Trespalacios, F. and Grossmann, I. E. (2014). Review of mixed-integer nonlinear and generalized disjunctive programming methods. *Chemie Ingenieur Technik*, 86(7):991–1012.

(16) Ye, Y., Grossmann, I. E., and Pinto, J. M. (2018). Mixed-integer nonlinear programming models for optimal design of reliable chemical plants. *Computers & Chemical Engineering*, 116:3–16.

(17) Ye, Y., Grossmann, I. E., Pinto, J. M., and Ramaswamy, S. (2019). Modeling for reliability optimization of system design and maintenance based on markov chain theory. *Computers & Chemical Engineering*.

(18) Young, P. and Zamir, S. (2014). *Handbook of game theory*. Elsevier.

(19) Zamarripa, M. A., Aguirre, A. M., Méndez, C. A., and Espuña, A. (2013). Mathematical programming and game theory optimization-based tool for supply chain planning in cooperative/competitive environments. *Chemical Engineering Research and Design*, 91(8):1588–1600.